NOTICE

The quality of this microform is heavily dependent upon the quality of the original thesis submitted for microfilming. Every effort has been made to ensure the highest quality of reproduction possible.

If pages are missing, contact the university which granted the degree.

Some pages may have indistinct print especially if the original pages were typed with a poor typewriter ribbon or if the university sent us an inferior photocopy.

Reproduction in full or in part of this microform is governed by the Canadian Copyright Act, R.S.C. 1970, c. C-30, and subsequent amendments.

AVIS

La qualité de cette microforme dépend grandement de la qualité de la thèse soumise au microfilmage. Nous avons tout fait pour assurer une qualité supérieure de reproduction.

S'il manque des pages, veuillez communiquer avec l'université qui a conféré le grade.

La qualité d'impression de certaines pages peut laisser à désirer, surtout si les pages originales ont été dactylographiées à l'aide d'un ruban usé ou si l'université nous a fait parvenir une photocopie de qualité inférieure.

La reproduction, même partielle, de cette microforme est soumise à la Loi canadienne sur le droit d'auteur, SRC 1970, c. C-30, et ses amendements subséquents.

Fractionation of Organic Liquid Mixtures by Reverse Osmosis

Yi Fang

A thesis
submitted to the School of Graduate Studies and Research
in partial fulfillment of the
requirements for the degree of
Master of Applied Science
in the Department of Chemical Engineering
the University of Ottawa

NOTICE

The quality of this microform is heavily dependent upon the quality of the original thesis submitted for microfilming. Every effort has been made to ensure the highest quality of reproduction possible.

If pages are missing, contact the university which granted the degree.

Some pages may have indistinct print especially if the original pages were typed with a poor typewriter ribbon or if the university sent us an inferior photocopy.

Reproduction in full or in part of this microform is governed by the Canadian Copyright Act, R.S.C. 1970, c. C-30, and subsequent amendments.

AVIS

La qualité de cette microforme dépend grandement de la qualité de la thèse soumise au microfilmage. Nous avons tout fait pour assurer une qualité supérieure de reproduction.

S'il manque des pages, veuillez communiquer avec l'université qui a conféré le grade.

La qualité d'impression de certaines pages peut laisser à désirer, surtout si les pages originales ont été dactylographiées à l'aide d'un ruban usé ou si l'université nous a fait parvenir une photocopie de qualité inférieure.

La reproduction, même partielle, de cette microforme est soumise à la Loi canadienne sur le droit d'auteur, SRC 1970, c. C-30, et ses amendements subséquents.

ISBN 0-315-60619-3

UNIVERSITÉ D'OTTAWA
UNIVERSITY OF OTTAWA

Abstract

A systematic investigation has been conducted to demonstrate the general applicability of reverse osmosis (RO) fractionation of organic liquid mixtures by laboratory prepared cellulose acetate butyrate (CAB) and aromatic polyamide (PA) membranes. Surface excess values have been determined by liquid chromatography (LC) technique for the four model organic liquid mixtures for CAB and PA materials.

The principal findings of this study are: (i) separations take place in all the four model organic liquid mixtures, and PA membranes give separations higher than CAB membranes under same experimental conditions; (ii) preferential sorption exists in all the four model systems for CAB and PA materials; (iii) the RO results are explained by the combined consideration of surface excess data determined from LC, and Stokes' Law radius calculated from literature data.

Acknowledgement

The author wishes to express his appreciation and gratitude to Professor T. Matsuura, National Research Council of Canada, Professor S. Sourirajan, Industrial Membrane Research Institute, Department of Chemical Engineering at the University of Ottawa, for their suggestions and guidance throughout this research project.

The principal financial support of Esso Petroleum Canada, under an Imperial Oil University Research Grant, and a URIF matching grant from the Government of Ontario (OT10-004), and also the partial support of NSERC, and the International Desalination Association and the School of Graduate Studies and Research of the University of Ottawa for the Award of Scholarship, are gratefully acknowledged.

The author also wishes to thank his parents and other family members for their help and encouragement during the course of this project.

Contents

List of Figures

List of Tables

Nomenclature

a	= activity of the solute, mol/m^3
A_P	= surface area of polymer powder in the chromatography column, m^2
c	= molar concentration, mol/m^3
c_A	= molar concentration of the component A in the binary mixture, mol/m^3
c_B	= molar concentration of the component B in the binary mixture, mol/m^3
$c_{A,b}, c_{B,b}$	= c_A *and* c_B in the bulk solution, mol/m^3
$c_{A,i}$	= c_A in the interfacial solution, mol/m^3
$\bar{c}_{A,i}$	= average value of $c_{A,i}$
D	= diffusivity coefficient, m^2/s, (cm^2/sec)
D_L	= diffusivity of solute at infinite dilution, m^2/s
D_{AB}	= diffusivity of component A in solvent B, m^2/s
f	= quantity defined by eq.37
k	= Boltzmann constant
K'_A	= equilibrium distribution coefficient of a solute defined by eq.3
M	= solvent molecular weight
r	= Stokes' Law radius, m
r_{AB}	= Stokes' Law radius of component A in solvent B, m
r_{BA}	= Stokes' Law radius of component B in solvnet A, m
R	= gas constant, Joule/((K)(mol))
T	= absolute temperature, K
t_a	= retention time of species a, minute
t_i	= thickness of interfacial solvent layer, m
V	= carrier solvent flow rate, cm^3/min

$\overline{V}_A, \overline{V}_B$ = average molar volume of the component A and the component B, respectively, m^3/mol

V_b = molar volume of solute at normal boiling point, m^3/mol

V_d = dead volume in a column, cm^3

V_m = volume of the mobile phase, cm^3

V_R' = retention volume, cm^3

V_s = volume of the stationary phase, cm^3

wt.% = weight percentage

X_A, X_B = mole fraction of the component A and the component B, respectively

X = association parameter defined by the Wilke-Chang equation

Greek Letters

Γ = surface excess, mol/m^2

Γ_A, Γ_B = Γ for the component A and for the component B, respectively, mol/m^2

γ = interfacial tension, N/m

μ = soluton viscosity, $N.s/m^2$,(centipoise)

ρ = density, kg/m^3

Subscripts

A	= solute or the component A in the binary mixture
B	= solvent or the component B in the binary mixture
b	= bulk phase
i	= interfacial phase
min	= minimum value

Superscripts

A	= the component A used as chromatographic solvent
B	= the component B used as chromatographic solvent
mixt	= the binary mixture of A and B used as chromatographic solvent

Chapter 1

1 Introduction

1.1 Separations and Chemical Engineering

Separation processes are at the technological heart of the chemical, polymer and energy industry. Literally thousands of products are concentrated, fractionated and/or purified to required purities and recoveries at reasonable prices. It is not an overstatement to maintain that our modern chemical and energy industries could not exist were it not for a highly developed portfolio of separation processes to handle the myriad of separation tasks required for producing these products. These products in turn are absolutely vital to our economic well-being [1].

In fact, there are virtually no major industries, not only the established ones but also the newest of the new, which are not impacted in some significant way by separation processes.

In this work, membrane separation process, in particular , reverse osmosis treatment of organic liquid mixtures is studied.

1.2 Membranes in Chemical Engineering

Membranes and membrane technologies have been categorized as one of the frontiers in chemical engineering in an investigation conducted by

National Research Council's Committee on Chemical Engineering Frontiers [2].

Membranes are thin two-dimensional structures designed to pass preferentially certain components [2]. Highly efficient separations of gaseous or liquid components can be achieved with such technologies as reverse osmosis,ultrafiltration,microfiltration, gas separations,dialysis,and electrodialysis. In these systems, membrane permeates are driven either by pressure, or by a gradient in chemical or electrochemical potential. Membranes are also finding increasing use in controlled drug release devices and biosensors. Traditional applications of membrane technologies have barely scratched the surface of an exciting and rapidly developing area.

On the material side,chemical engineers can make important contributions to the development of new materials—which is one of the components of this thesis, the engineering of structure or morphology into membranes, and the identification of new ways of using permselective membranes.

On the application side, integrated membrane processes represent an attractive area to be developed, in which a membrane separation is combined with a conventional separation method to accomplish a job neither process by itself could do. Examples, like the distillation of azeotropic mixtures, the use of hollow fiber membranes in bioreactors, and the combination of a permselective membrane with a catalytic membrane, have been reported in the literature [2].

In brief, despite being young compared with other unit operations, membranes and membrane technologies have been enjoying an increased popularity in various aspects of chemical engineering and have much more

space to grow. Fig. 1 is a good indication of the above point of view.

1.3 Separation of Organic Liquids by Membrane–RO process

1.3.1 State-of-the-art

The separation of organic liquid mixtures by the reverse osmosis membrane process is of practical interest from the point of view of finding a separation process alternative or compatible to the conventional distillation process,and/or other separation methods presently used.

Even though the applicability of reverse osmosis for the separation of organic liquid mixtures was demonstrated in principle as early as 1964 [3], and it is particularly useful for upgrading organic liquid mixtures encountered in the petroleum industry [4], the process has not yet gained entry into the general petroleum and petrochemical industry to any significant extent, and many of the fundamental studies needed to make such entry the most effective and profitable have not yet been made, mainly because of the instability of the porous structure of the available membranes in the nonaqueous solution environments encountered in practice.

1.3.2 Necessity

Despite the apparent proliferation of membrane processes, the science and technology of industrial membranes is still in its early stages of development. So is that of RO applications in nonaqueous systems.

As for industry practice, membrane science and technology is also ranked as relatively new as it can be seen from Figure 1 showing that

RESULTS OF POLL ON TECHNOLOGICAL AND USE MATURITIES OF SEPARATION PROCESSES

Process	Technological Maturity*	Use Maturity*
Distillation	87	87
Extractive/Azeotropic Distillation	80	65
Solvent Extraction	73	61
Gas Absorption	81	76
Supercritical Gas Absorption/Extraction	28	25
Adsorption: Gas Feed	57	52
Adsorption: Liquid Feed	50	40
Ion Exchange	60	60
Membranes: Gas Feed	39	27
Membranes: Liquid Feed	37	30
Liquid Membranes	13	13
Chromatography: Liquid Feed	30	22
Affinity Separations	15	9
Crystallization	64	62
Electrical and Other Field-Induced Separations	24	13

*Scores respresent the averages of the percentages of the distances to the technological or use asymptote, i.e., a score of 100 would denote that a given process has reached an asymptote.

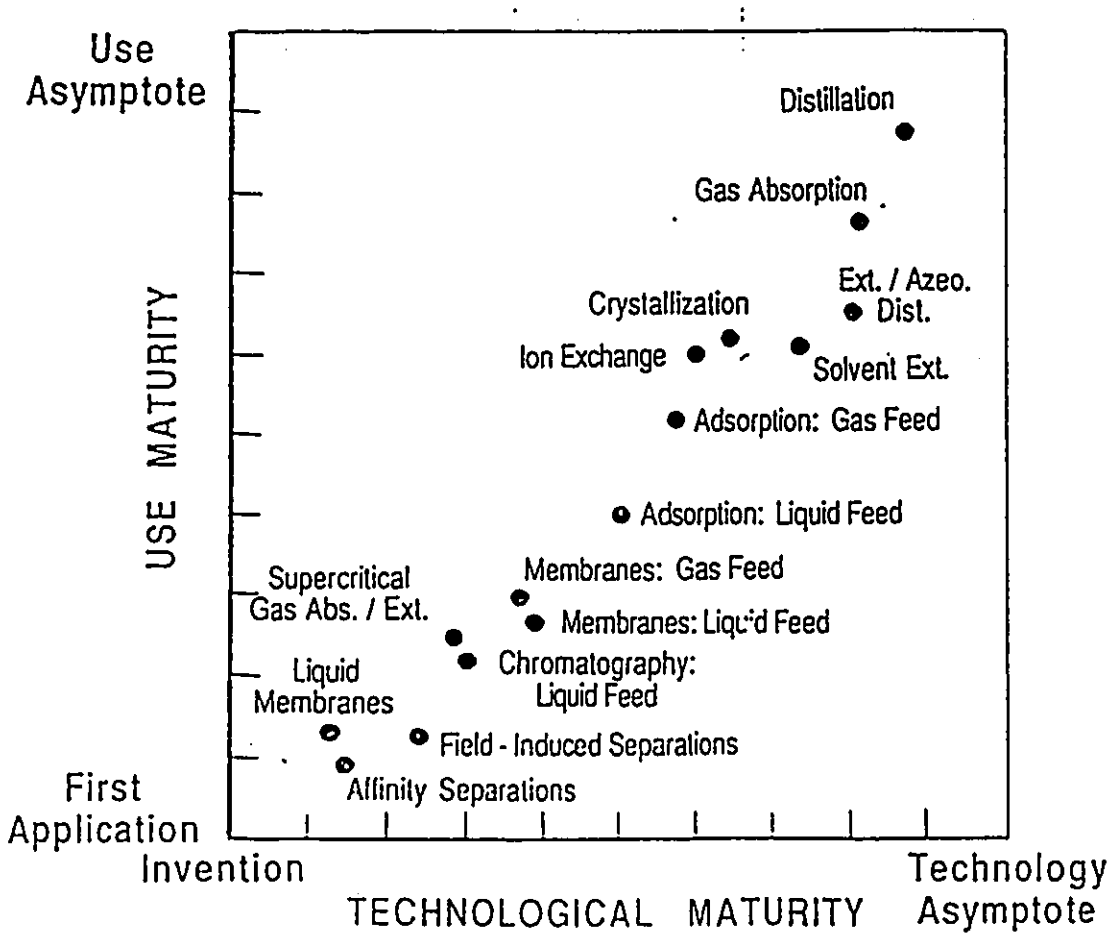

Figure 1: Technological and use maturities of separation processes.

membrane process has about 30% maturity compared with distillation's 87% maturity. As one of the many membrane processes today, RO also has more space to be explored and the separation of organic liquid mixtures by reverse osmosis is one of the multitudes of potential applications.

Therefore, it can be obviously concluded that there is a genuine need in the development of reverse osmosis for the nonaqueous treatment, in particular, the separation of organic liquid mixtures.

1.3.3 Purpose of This Work

This work is a systematic approach which serves three major purposes:

1. Further feasibility studies of the technique for the RO treatment of organic liquid mixtures.

2. Further investigation of membrane performances in the environments of organic liquid mixtures.

3. Interpretation of membrane performances with the physicochemical data generated from this work.

1.3.4 How This Study is Conducted

To conduct this study, the author investigates, firstly, how membranes perform in the organic liquid mixtures, and secondly, why these membranes perform so.

1.3.5 The Significance and Potentiality of This Work

This work can make a significant scientific contribution and lead to significant technological developments for new processes and products in the area mentioned above. They are of major economic significance to

petroleum, petrochemical and energy related biomass conversion industries.

The potentiality of this work is well expressed in the potentiality of RO treatment of organic liquid mixtures. Tremendous opportunities exist for the penetration of RO technique into every aspect of nonaqueous applications. Dramatic increase worldwidely of level of research and development activity in this field indicates both the growing recognition of the commercial potentialities of membrene separations, and the growing realization of the international scientific and engineering community that membranes are capable of playing tremendously beneficial roles in society and industry far more than what has hitherto been appreciated.

1.4 Application of Liquid Chromatography Method in Membrane Studies[5-6]

The interaction forces working at the polymer-solution interfacial region can be simulated by a liquid chromatography system in which the column is packed by the polymer from which the membranes are made, and the solute is injected into the solvent stream.

Since the interaction forces prevailing at the membrane-solution interface during reverse osmosis may be considered to be analogous to those working in the system solute-solvent-column polymer material in liquid chromatography, and the magnitude of the above interactions are explicitly exhibited in the retention volume data of the corresponding chromatography experiments,liquid chromatography offers a powerful tool to better understand the physicochemical nature of RO separations and to provide with scientific foundation for membrane performance prediction and sub-

sequently for membrane design.

Details of LC applications in this study will be presented in the later chapters.

Chapter 2

2 Literature Survey

2.1 An Overview

It has been recognized that the instability of the porous structure of the membranes accounts for reverse osmosis (RO) not gaining entry into the general organic chemical industry. Despite the increasing awareness of RO's nonaqueous applications, current literature on this subject is neither extensive nor intensive, compared with aqueous applications.

Many of that little available information appears in patents because of the technological reason of RO technique. There has been clear evidence, especially in recent years, that the concept [7] is gaining popularity that RO is not limited to the treatment of aqueous solutions, and that it is equally applicable for the treatment of nonaqueous solutions in liquid phase. Table 1 is a summary of a recent patent survey. It can be seen from Table 1 that the number of patents on this subject increases dramatically from 1960's to recent years, which is a good indication of increasing research work in this field.

2.2 Previous Work

The interesting innovation of RO for the separation of organic liquids was first conducted and illustrated in principle by Sourirajan in 1964 [3]. Sourirajan had separated xylene-ethanol, xylene-heptane mixtures and

Table 1: Institutions and their patents for RO in nonaqueous fields

Institution	Source	Year
Shell International Research Maatschappij B.V.	GB Appl.85/21,607	1985
	Eur.Pat. Appl.EP254,359	1988
Canadian Patents and Development Ltd.	Can.CA Appl.489,596	1985
Signal Res. Cent.Inc., U.S.A.	AIChE Symp. Ser.	1986
Imperial Oil Ltd.	Can.CA 1,215,328	1986
UOP Inc.	U.S.US 4,617,126	1986
	U.S.US 4,595,507	1986
Monsanto Co.	UK Pat. Appl. GB 2169301	1986
Tokyo Inst. Technol. Yokohama, Japan	J.Chem.Eng. Japan	1986
Daicel Chemical Industries, Ltd, Japan	Jpn. Kokai Tokkyo Koho JP 61 36,399	1986
Sagami Chemical Res. Center, Japan	Eur. Pat. Appl. EP 190,647	1986
Sasakura Engineering Co., Ltd., Japan	Jpn. Kokai Tokkyo Koho Jp 63 69,507	1988
Standard Oil Company, U.S.A.	U.S.US 3,140,256	1964
Exxon Research & Engineering Co.	Eur. Pat. Appl. 160,140	1985
	Eur. Pat. Appl. 160,142	1985
	U.S. US 4,541,972	1985
	U.S. US 4,496,456	1985
	U.S. US 4,510,047	1985
	U.S. US 4,477,333	1984
	U.S. US 4,368,112	1983
	U.S. US 4,715,960	1987
	Eur. Pat. Appl. EP 145,127	1985

their azeotropic mixtures by using a static cell with cellulose acetate and polyethylene films.

Kopecek and Sourirajan had reported more data on the separation of binary azeotropic mixtures, and isomers in 1969-70 [8,9].

In 1983 , Adam, Luke and Meares [10] published the results of their studies on this topic, focusing on exploring the factors governing the selectivity coefficient.

Farnand, Talbot, Matsuura and Sourirajan have extended their work and further illustrated the applicability of the RO technique for the separation of organic liquid mixtures in their reports during 1980-84 [11-13].

In 1986, Kulkarni, Funk and Li [14] reported hydrocarbon separations with polymeric membranes.The hydrocarbons separated are chemically similar but differ significantly in molecular weight.

2.2.1 Membrane R & D for Nonaqueous Applications

Since ordinary reverse osmosis membranes cannot resist the attack by organic compounds, it has been the focus of membrane and membrane material research and development to overcome this deficiency.

As one approach, plasticization of membranes by solutes is being studied extensively, i. e. in the Separation Research Program at the University of Texas, Austin, which is devoted to the understanding of the solute-membrane-solvent interaction relevant to plasticization [15].

Other approaches have also been made. Membranes made from various materials, such as, novel cellulose, modified polysolfone, aromatic polyamide, polyimide,polycarbonate, cellulose acetate, cellulose acetate bu-

tyrate,copolymer, and inorganic glass membranes have been reported by different research groups [16-26] with various applications. It has also been found that there are more and more reports/patents concentrated on two areas basically—hydrocarbon separation industry and oil refining processes.

2.2.2 Material Systems Studied

In general, the treated material systems include separations and purification of aliphatic hydrocarbons,aromatic hydrocarbons, aliphatic-aromatic hydrocarbons, alcohols, isomers, azeotropes, emulsions and so on.

In detail, some of these material systems are separation of butadiene and pentadiene, separation of methyl benzene and 1-hexadecene, separation of m-xylene from o-xylene, to separate polar organic solvent from dewaxed oil, solvent recovery in lubricating oil dewaxing etc.

2.3 Models for Transport through Membranes

2.3.1 Various Models Suggested

Several approaches have been made towards understanding the basic transport mechanisms, namely, Irreversible Thermodynamics Model, Finely-Porous Model, Solution-Diffusion Model, Surface Force-Pore Flow Model, etc. Most of these approaches, however, fall into two categories, porous and non-porous. In the first case, the membrane is considered as a bundle of capillaries where the flow is determined by the application of Poiseuille's equation. The other case involves dissolution of the components in the membrane followed by diffusion through the membrane [27]. These principal approaches and the extent of their usefulness are discussed

as follows.

Irreversible Thermodynamics Model

The first practical model was developed by Kedem and Katchalsky [28] . This model was for transfer of non-electrolytes through membranes and was extended to electrolytes. It is an elegant model and works well when the structure of the membrane is not known and the molecular mechanisms of transport processes within the membrane are not fully understood [29]. The parameters, however, are not related to any physical characteristics, since this approach treats the membrane as a "black box ".

Solution-Diffusion Model

This model was developed by Lonsdale et al [30]. In this model, transport processes are regarded as being governed by two factors, thermodynamic property— solubility and dynamic property—diffusivity, which control permeability. The solute and the solvent dissolve in the membrane by diffusion through the homogeneous nonporous surface layer. The solubility and diffusivity of solvent and solute are two important parameters in this model. The problem with this model is that it does not consider the structure of the membrane. It also breaks down for high concentrations of solutes. Yet it is the most used model in module design due to the simplicity of the calculations necessary. And it gives a reasonable estimation.

Finely-Porous Model

This model assumes a porous membrane structure. Jonsson and Boesen [31] combine diffusion with viscous flow through the pores. It is more complicated than the Solution Diffision Model since it uses three parameters. An average pore size can be calculated from this model.

2.3.2 Surface Force-Pore Flow Model

The reason that this model is discussed separately from others is that the majority of the analysis and interpretation of many experimental results in this work is based on this model.

The Surface Force Pore Flow Model was first presented by Matsuura and Sourirajan [32]. Briefly, the model can be described as follows. The membrane is assumed to be microporous and the pores are modelled as perfect cylinders, with or without a pore size distribution. A two-dimensional approach is used (see Figure 2) so that the solute velocity and concentration in the pore vary in both radial, r, and axial, z, directions. A balance of applied and frictional forces acting on the solute in the pore is given as a function of the radial and axial positions. The solute-membrane interactions are expressed by a Sutherland-type potential function. A friction parameter, b(r), which is the ratio of solute diffusivity in free solution to solute diffusivity inside a pore, is used to describe the hydrodynamic drag on the solute by the pore wall. Initially it was suggested that the friction parameter was a function of radial position [32]. However, b was treated as a constant in the later papers [33,34].

This model considers both the nature of the solution as well as that of the surface in contact. From this model, reverse osmosis is regarded as the combined result of preferential sorption of one of the constituents of the feed solution at the membrane-solution interface, and mass transport by fluid permeation under pressure through the capillaries of the microporous membrane. An appropriate physicochemical nature of the membrane sur-

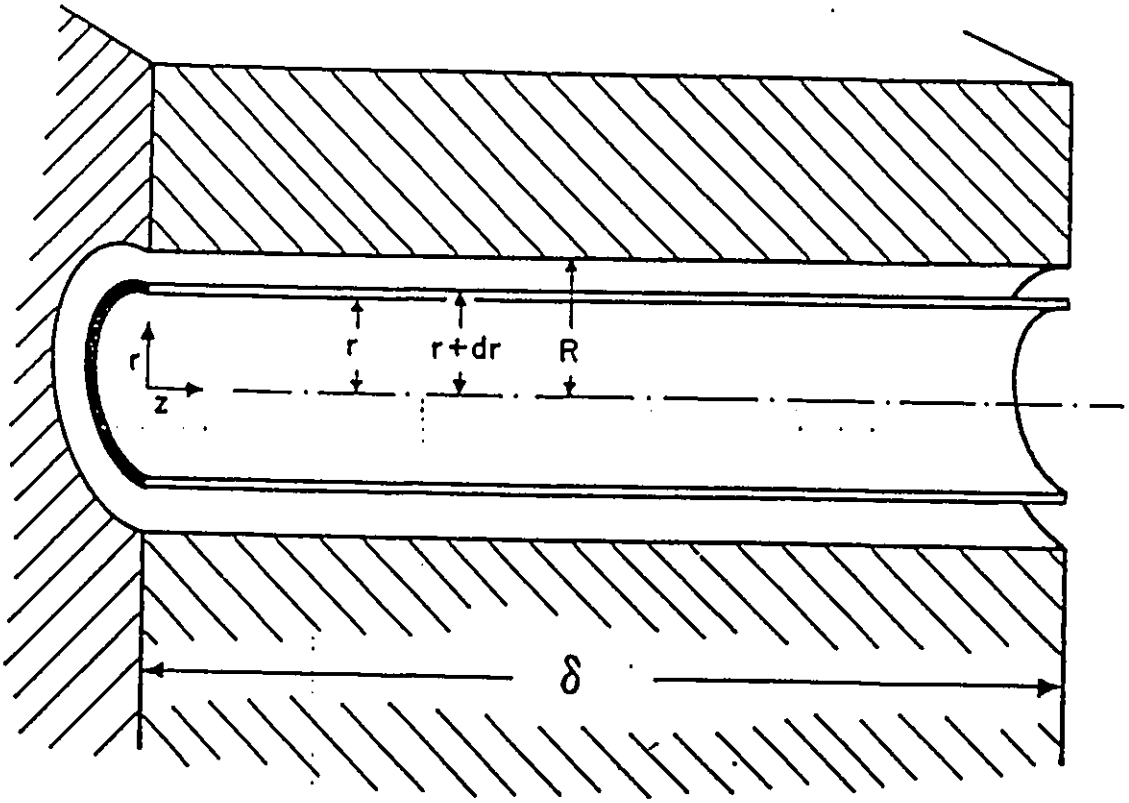

Figure 2: Cylindrical coordinates in a membrane pore.

face and the physical structure in terms of the appropriate number and size of pores are needed for a practical separation process. It is more elaborate and complicated, since this model explains the mechanism more fully than the above ones, and subsequently, it requires more parameters to describe the mechanism [29].

It has to be noted that Mehdizadeh and Dickson [35] recently suggested a modified Surface Force Pore Flow Model whose major difference from Surface Force Pore Flow Model is the different approach to the calculation of velocity profile. There is no further comment on this modification since this series of papers has not been fully published yet.

Chapter 3

3 Application of Liquid Chromatography Method in Membrane Separation Studies on Binary Organic Liquid Mixtures

This chapter explains why LC method is used and how it is applied to this study. The conventional LC theory applicable to the dilute solution system is briefly outlined first. Then, it is expanded to a system involving binary mixtures of organic liquids.

3.1 Analog of LC System to Membrane Separation Process

3.1.1 Liquid Chromatography: An Introduction

Chromatography is a term applied to all techniques which enable the separation of chemical mixtures by exploiting the phenomenon of differential migration as a solution passes through a column. A carrier fluid containing a mixture is passed over a bed of porous material. Each component of the mixture has its own distinct physical and chemical properties resulting in different rates of migration for each individual element. This idea of different rates of movement for components of a solution through a packing is applicable regardless of the phase of the solution or the nature of the packed bed. Chromatography can be subdivided into gas-solid chromatog-

raphy, gas-liquid chromatography and liquid-solid chromatography.

The liquid chromatography system consists of a carrier liquid (solvent),various components (solutes) dissolved in the liquid as well as porous support. There is a distribution of components in the fluid between a mobile and a stationary phase due to the presence of the packing material. This distribution results from the difference in adsorption potential of the solute and solvent as well as the difference in interaction energies between the mobile and stationary phases.

3.1.2 Analog of Liquid Chromatography System to a Membrane Separation Process

There is a direct relationship (see Figure 3) between the physicochemical processes occurring in a liquid chromatography system and those at the membrane-solution interface. Both systems are concerned with the behavior of a surface-influenced liquid layer.

This layer is known as the stationary phase in LC terms, while for membrane systems the term interfacial layer is used. The mobile phase in a LC system is analogous to the bulk solution of a membrane system. The introduction of a solute in either system results in a concentration difference between the mobile (bulk) phase and stationary (interfacial) phase. This differential concentration results in a retention time difference in the case of a liquid chromatograhpy system, and produces positive and negative concentration gradients at the membrane-solution interface.

Due to the similarities between the two systems, the solute concentration on the surface of a membrane can be obtained by relating the interfacial behavior to quantitative values obtained in a LC system. The nature and strength of the interactions between the solute and the membrane are reflected in the retention time (t_a) of the solute (a) in a liquid chromatography column. A relative scale can be set up to compare the interactions. The result can be interpreted as follows: Suppose the retention time for solute c (t_c) is greater than the retention time for solute d (t_d), this means the polymer has a greater affinity for c than d. Therefore, if the polymer is to be made into a membrane, we can say that the separation process based on the rejection of d and the permeation of c is thermodynamically favorable.

3.2 Expansion of LC Theory for the Dilute Solution System to the One Applicable to Binary Mixtures of Organic Liquids

3.2.1 Conventional LC Theory Applicable to the Dilute Solution System

The core concepts in the classic LC theory are retention time and retention volume. The retention time describes the passage of a solute through any chromatographic column under the influence of the packing [37]. Since the retention time varies inversely as the carrier flow rate (V), an expression for this value, independent of system dimensions,is to characterize retention behavior in terms of the volume flow between injection of the solute into

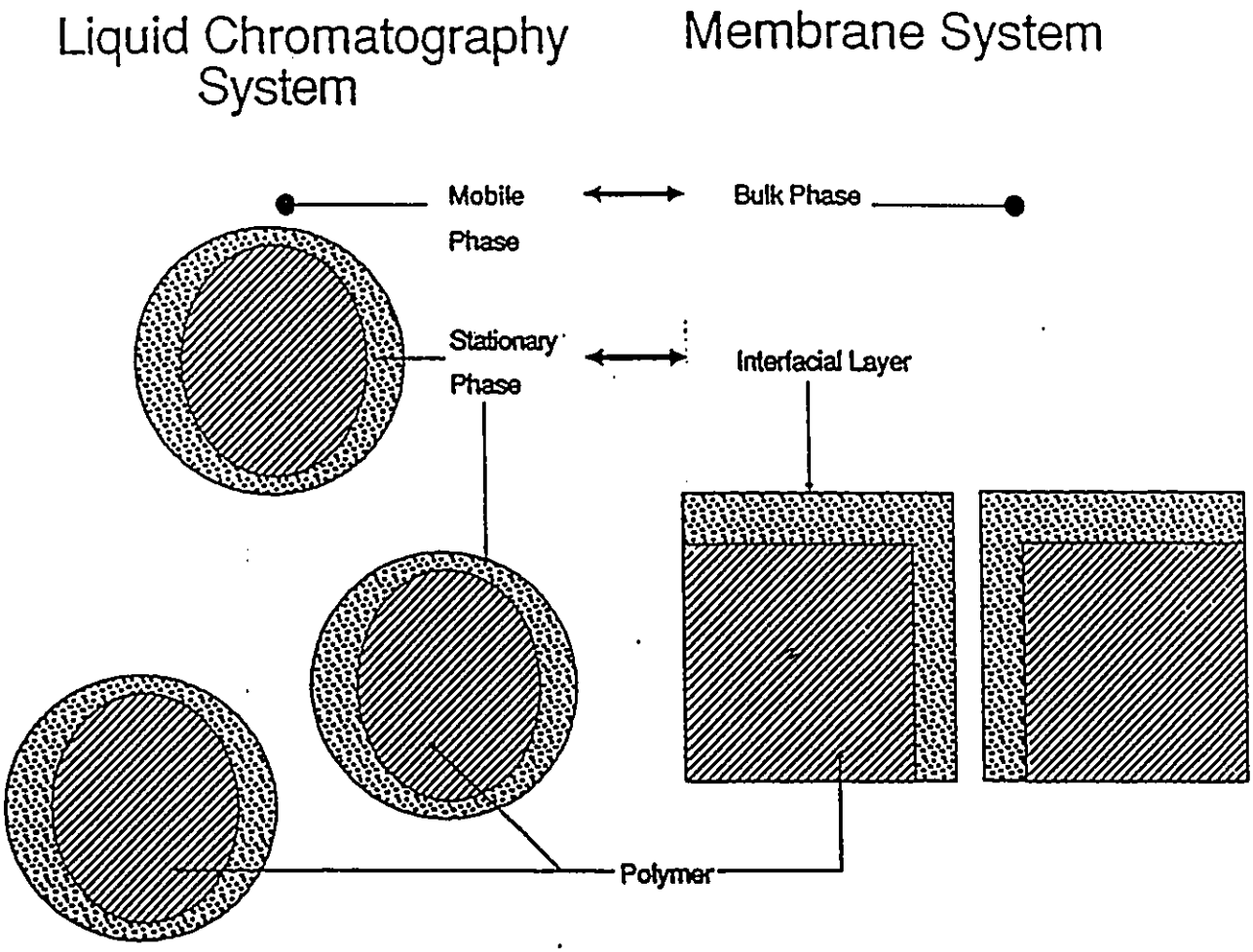

Figure 3: Relationship between a liquid chromatography system and a membrane system.

the column and the emergence of a maximum concentration of the solute at the end of the system [38]. This value is known as the retention volume V'_R;it can be obtained by multiplying the retention time by the volumetric flow rate (V).

$$V'_R = t_a V \tag{1}$$

The retention volume V'_R of solute (A) from any chromatography system contains the contribution of the mobile phase (V_m),the stationary phase (V_s) as well as a quantity known as the system dead volume (V_d).The experimental retention volume is the sum of the various contributions:

$$V'_R = V_m + V_d + K'_A V_s \tag{2}$$

The system dead volume can be defined as the volume in a chromatographic system which does not contribute to the retention time of the solute due to surface interactions. The system dead volume is caused by connecting tubings,fittings, refractometer cells, etc.

Further,

K'_A,equilibrium distribution coefficient for the solute,is defined as

$$K'_A = \frac{concentration\ of\ solute\ A\ in\ the\ interfacial\ solvent\ phase}{concentration\ of\ solute\ A\ in\ the\ bulk\ solvent\ phase} \tag{3}$$

It should be noted here that, in the analog of LC system to a membrane separation process, the concentration of solute A in the *stationary* phase is simulated and regarded as the same as that in the *interfacial* solvent phase. So is the relation between the concentration of solute A in the *mobile* solvent phase and the in the *bulk* solvent phase.

3.2.2 Theory Development

Determination of Surface Excess for the Dilute Solutions

In order to determine the values of V_s and K'_A,the following assumptions are made:

(i) $K'_A = 1$ for pure solvent (B), which means that the probability of any solvent molecule to exist in the mobile phase is the same as that in the stationary phase. When $K'_A = 1$, let

$$V'_R = [V'_R]_B = V_m + V_d + V_s \tag{4}$$

(ii) $K'_A = 0$ for a reference solute with the lowest retention volume. This means that such a reference solute is so strongly repelled from the surface of the polymer material at the interface that the reference solute stays only in the mobile phase of the column. Hence the concentration of the reference solute in the interfacial solvent layer can be assumed zero, i.e., the distribution coefficient of solute A is zero, when $K'_A = 0$, let

$$V'_R = [V'_R]_{min} = V_m + V_d \tag{5}$$

From eq. 4, 5,

$$V_s = [V'_R]_B - [V'_R]_{min} \tag{6}$$

Combining eq. 4, 5, and 6,

$$K'_A = \frac{V'_R - [V'_R]_{min}}{[V'_R]_B - [V'_R]_{min}} \tag{7}$$

If A_P is the total effective surface area of the polymer in the chromatographic column, then the thickness t_i of the interfacial solvent layer

is:

$$t_i = V_s/A_p \tag{8}$$

Let the average concentration of solute at the interface as $\overline{c}_{A,i}$, and the concentration of solute in the bulk solution phase as $c_{A,b}$, eq. 3 becomes

$$K'_A = \overline{c}_{A,i}/c_{A,b} \tag{9}$$

The surface excess with the thickness of the interfacial layer, t_i , is the concentration difference between the bulk ($c_{A,b}$) and the interface ($\overline{c}_{A,i}$)[7].

$$\Gamma/t_i = \overline{c}_{A,i} - c_{A,b} \tag{10}$$

Combining eq. 9, 10:

$$\Gamma/t_i = c_{A,b}K'_A - c_{A,b} \tag{11}$$

or

$$\frac{\Gamma}{c_{A,b}} = (K'_A - 1)t_i \tag{12}$$

Substituting eq. 7, 8, 6 into eq. 12, and noticing $[V'_R] = [V'_R]_{soluteA}$,

$$\begin{aligned} \frac{\Gamma}{c_{A,b}} &= \left(\frac{[V'_R] - [V'_R]_{min}}{[V'_R]_B - [V'_R]_{min}} - 1\right)\left(\frac{[V'_R]_B - [V'_R]_{min}}{A_P}\right) \\ &= \frac{[V'_R]_{soluteA} - [V'_R]_B}{A_P} \end{aligned} \tag{13}$$

or

$$\frac{\Gamma_A}{c_{A,b}} = \frac{[V'_R]_A - [V'_R]_B}{A_P} \tag{14}$$

Subscripts A and B refer to solute and solvent, respectively. Up to here, the theory of obtaining surface excess using retention volume data from liquid chromatography experiment has been established for the dilute

solution. In the next section, the surface excess is determined for the binary mixtures in the entire composition range.

Determination of Surface Excess in Binary Mixture of Organic Solvents—Theory Development

The theory [40,14] outlined below was developed on the assumption that the surface area of the polymer utilized for sorption of both components is independent of the solution composition.

The surface excess of the component A, regarded as solute in solvent B, equation 14 can be rewritten as

$$\Gamma_A/c_{A,b} = ([V_R']_A^B - [V_R']_{B,pure}^B)/A_P \qquad (15)$$

where $[V_R']_A^B$ is the retention volume of the component A and $[V_R']_{B,pure}^B$ is the retention volume of solvent B. The superscript B indicates that the component B is used for the solvent in this chromatographic experiment. For obtaining the above surface excess the following liquid chromatographic experiment has to be conducted.

The chromatography column is packed with the powder of the polymeric material which shall be used for the membrane separation. Pure solvent B is pumped through the column and the solution of A in B is injected at the column inlet as a sample and the retention volume $[V_R']_A^B$ is measured. Then, a solution of deuterated isotope of the component B in solvent B is injected and the retention time is recorded as $[V_R']_{B,pure}^B$. The surface area of the polymer packed in the column,A_P, can be measured independently by gas chromatography method [41,42,43]. In analogy to eq.15 we obtain the specific surface excess of the component B in the solvent A

as

$$\Gamma_B/c_{B,b} = ([V_R']_B^A - [V_R']_{A,pure}^A)/A_P \tag{16}$$

where $[V_R']_B^A$ is the retention volume recorded when a solution of B in solvent A is injected at the column inlet and $[V_R']_{A,pure}^A$, is the retention volume recorded when a solution of the deuterated isotope of component A in the solvent A is further injected. The superscript A indicates that the solvent stream through the column is switched from pure solvent B to the pure solvent A in the above chromatographic experiment.

In the next liquid chromatography experiment the solvent stream is switched to the mixture of component A and component B, with concentrations of $c_{A,b}$ and $c_{B,b}$ respectively. The subscript b indicates the concentration of the bulk solution, which is the same as that of the solution flowing through the column.The component A and the component B are injected at the column inlet and the retention volumes $[V_R']_A^{mixt}$ and $[V_R']_B^{mixt}$ are measured and recorded. In analogy to eqs.15 and 16 we can obtain the surface excess of the component A and the component B by

$$\Gamma_A/c_{A,b} = ([V_R']_A^{mixt} - [V_R']_{mixt}^{mixt})/A_P \tag{17}$$

$$\Gamma_B/c_{B,b} = ([V_R']_B^{mixt} - [V_R']_{mixt}^{mixt})/A_P \tag{18}$$

Again, the superscript mixt indicates that a binary mixture of the component A and the component B is supplied into the column as a chromatography solvent. The retention volume $[V_R']_{mixt}^{mixt}$ is an imaginary quantity indicating the retention volume of the binary mixture of the component A and the component B, which is regarded as one single phase.

Among quantities involved in eqs. 17 and 18 the following relations hold:

$$c_{A,b}\overline{V}_A + c_{B,b}\overline{V}_B = 1 \tag{19}$$

$$\Gamma_A\overline{V}_A + \Gamma_B\overline{V}_B = 0 \tag{20}$$

In eq.19 $c_{A,b}\overline{V}_A$ and $c_{B,b}\overline{V}_B$ indicate the volume fraction of the component A and that of the component B, respectively, in the mixture thereof, and therefore,the sum is equal to unity. Equation 20 means that the volume fraction gained by the excessive amount of the component A at the interface is equal to the volume fraction lost with respect to the other component.

From eqs.17 and 18,

$$\Gamma_A\overline{V}_A = ([V_R']_A^{mixt} - [V_R']_{mixt}^{mixt})c_{A,b}\overline{V}_A/A_P \tag{21}$$

$$\Gamma_B\overline{V}_B = ([V_R']_B^{mixt} - [V_R']_{mixt}^{mixt})c_{B,b}\overline{V}_B/A_P \tag{22}$$

Adding eqs. 21 and 22 and using eq.20 we obtain:

$$\begin{aligned} &([V_R']_A^{mixt} - [V_R']_{mixt}^{mixt})c_{A.b}\overline{V}_A/A_P \\ = \; &-([V_R']_B^{mixt} - [V_R']_{mixt}^{mixt})c_{B,b}\overline{V}_B/A_P \end{aligned} \tag{23}$$

Rearranging:

$$\begin{aligned} &[V_R']_{mixt}^{mixt}(c_{A,b}\overline{V}_A + c_{B,b}\overline{V}_B) = \\ &[V_R']_A^{mixt}c_{A,b}\overline{V}_A + [V_R']_B^{mixt}c_{B,b}\overline{V}_B \end{aligned} \tag{24}$$

Using eq. 19:

$$[V_R']_{mixt}^{mixt} = [V_R']_A^{mixt}c_{A,b}\overline{V}_A + [V_R']_B^{mixt}c_{B,b}\overline{V}_B \tag{25}$$

It has to be noted that eq. 19 applies in the bulk phase while eq. 20 applies in the interfacial phase. Strictly speaking, the molar volumes of the component A and the component B are different numerically in the bulk and in the interfacial phase. But average molar volumes are used in this derivation and they are assumed to be constant either in the bulk or in the interfacial solution.

Equation 25 being inserted into eq. 17:

$$\begin{aligned}\Gamma_A/c_{A,b} &= ([V_R']_A^{mixt} - [V_R']_A^{mixt} c_{A,b}\overline{V}_A \\ &\quad -[V_R']_B^{mixt} c_{B,b}\overline{V}_B)/A_P \end{aligned} \tag{26}$$

Using eq. 19:

$$\Gamma_A/c_{A,b} = ([V_R']_A^{mixt} c_{B,b}\overline{V}_B - [V_R']_B^{mixt} c_{B,b}\overline{V}_B)/A_P \tag{27}$$

and

$$\Gamma_A/c_{A,b} = \frac{c_{B,b}\overline{V}_B([V_R']_A^{mixt} - [V_R']_B^{mixt})}{c_{A,b}\overline{V}_A + c_{B,b}\overline{V}_B}/A_P \tag{28}$$

Dividing both the numerator and the denominator of eq. 28 by the total molar concentration of the bulk solution:

$$\Gamma_A/c_{A,b} = \frac{X_{B,b}\overline{V}_B([V_R']_A^{mixt} - [V_R']_B^{mixt})}{X_{A,b}\overline{V}_A + X_{B,b}\overline{V}_B}/A_P \tag{29}$$

Likewise,

$$\Gamma_B/c_{B,b} = \frac{X_{A,b}\overline{V}_A([V_R']_B^{mixt} - [V_R']_A^{mixt})}{X_{A,b}\overline{V}_A + X_{B,b}\overline{V}_B}/A_P \tag{30}$$

It is noted that when pure B is used as a chromatography solvent $X_{A,b} = 0, X_{B,b} = 1, [V_R']_A^{mixt} = [V_R']_A^B$ and $[V_R']_B^{mixt} = [V_R']_{B,pure}^B$, and therefore eq. 29 is reduced to eq. 15.

Actual chromatography experiments are conducted as follows. A mixture of solvent A and B of known composition is pumped into the column as a chromatography solvent.Then,pure A and pure B are injected into the solvent stream as chromatography samples and retention times $[V_R']_A^{mixt}$ and $[V_R']_B^{mixt}$ are recorded corresponding to the given solution composition. Surface excess values are calculated from the experimental retention volume data.Thus the surface excess can be obtained in the entire composition range of the binary mixtures.

For the convenience of calculation, eq. 29 is converted as follows.

Noting $c_{B,b} = cX_{B,b}$, inserting into eq. 19:

$$c_{A,b}\overline{V}_A + cX_{B,b}\overline{V}_B = 1 \tag{31}$$

Dividing through by $c_{A,b}$:

$$\overline{V}_A + \frac{c}{c_{A,b}}X_{B,b}\overline{V}_B = \frac{1}{c_{A,b}} \tag{32}$$

Noting $c/c_{A,b} = 1/X_{A,b}$:

$$\overline{V}_A + \frac{1}{X_{A,b}}X_{B,b}\overline{V}_B = \frac{1}{c_{A,b}} \tag{33}$$

or

$$\frac{X_{A,b}\overline{V}_A + X_{B,b}\overline{V}_B}{X_{A,b}} = \frac{1}{c_{A,b}} \tag{34}$$

Inserting eq. 34 into eq. 29 and multiply $\overline{V}_A$ on both sides:

$$\Gamma_A A_P \overline{V}_A = \frac{X_{A,b}X_{B,b}\overline{V}_A\overline{V}_B([V_R']_A^{mixt} - [V_R']_B^{mixt})}{(X_{A,b}\overline{V}_A + X_{B,b}\overline{V}_B)^2} \tag{35}$$

From eq. 20:

$$\Gamma_B A_P \overline{V}_B = -\Gamma_A A_P \overline{V}_A \tag{36}$$

Eq. 35 is the final equation that is used in the calculation.

Chapter 4

4 Experimental Methods

4.1 Membrane Preparation Details

4.1.1 Cellulose Acetate Butyrate (CAB) Membranes

The film casting solution had the following composition (weight%):

cellulose acetate butyrate$(CAB-171-40)$:	14.0
acetone :	74.0
water :	9.0
magnesium perchlorate	3.0

Water was first added into a bottle equipped with a magnetic stirrer. Magnesium perchlorate was then added and fully dissolved in the water. Then acetone was added and mixed in the bottle. A colorless, transparent solution was formed. Afterwards CAB-171-40 (see Figs. 4 and 5 for details) was gradually added into this solution until all the polymer powder was added into the bottle. It took about 24 hours for all the CAB powder to be fully dissolved. Thus, a transparent casting solution was obtained.

The film was cast, by using the casting solution, on a glass plate with 0.025 cm (0.01 inch) side runners to give this thickness to the as-cast film. Uniformity of film thickness was obtained by passing a thick glass rod across the top of the plate, the glass rod resting on the side runners only.

The acetone was then allowed to evaporate at room temperature (23-25°C) from the surface of the film on the glass plate for a period of one

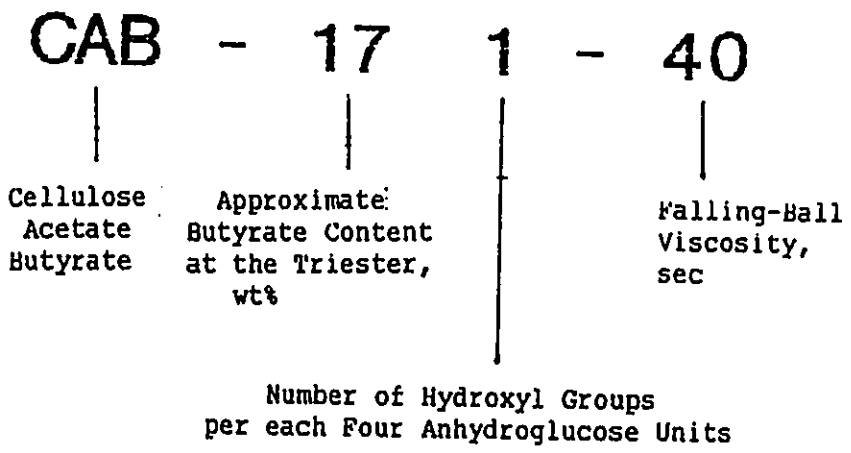

Figure 4 : Cellulose acetate butyrate code designation

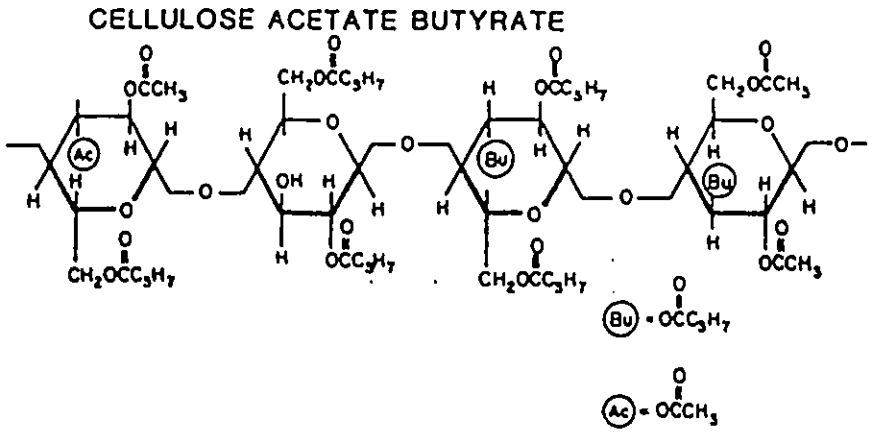

Figure 5: Chemical structure of cellulose acetate butyrate[45].

minute. This step in the film casting technique is generally referred as the evaporation step. During this step, the film also partially hardened to a semisolid mass.

The glass plate containing the partially hardened film was then carefully immersed into ice cold water in a tray where it was left at that temperature overnight. This step in the film casting technique is generally referred as the gelation step. During this step, the film finally set to a hard porous gel from which acetone and magnesium perchlorate were leached out practically completely. On standing in ice cold water overnight, the film peeled itself off, or could be removed by hand easily, from the surface of the glass plate. Then, the plain membrane was cut into coupons by punching a round knife on the surface of the plain membranes.

These membrane coupons were proceeded to next step–pretreatment.

Pretreatment here was referred to a temperature and pressure treatment before membranes' use in the reverse osmosis experiment. The temperature treatment consisted of shrinking the membrane held freely between two Pyrex petri dishes immersed in distilled water which was heated gradually from the laboratory temperature of 23-25°C to the required temperature 70°C and held at 70°C for 10 minutes. Then the film shrinkage process is terminated by transferring the film from hot water to the relatively colder laboratory temperature water. Heat-treated membranes were kept at all times in a glass bottle containing distilled water covering the membranes. The distilled water in the bottle was replaced with fresh distilled water every three days. The pressure treatment consisted of feeding distilled water over the surface of the film mounted in the reverse osmosis

cell at a pressure of 5517 kPag (800 psig) from compressed nitrogen gas for 2 hours, after which time it was released to atmosphere. This process is usually referred as pressurization.

4.1.2 Aromatic Polyamide (PA) Membrane

PA membranes used in the experiments were prepared using the following procedure. The aromatic polyamide powder was obtained from the Division of Chemistry, National Research Council of Canada, with the following characteristics: Number Averaged Molecular Weight = 31300, intrinsic viscosity in 96% sulfuric acid at 20 $°C$ = 1.80 dl/g, and the structure shown in Fig. 6.

The polyamide material was dried under vacuum at 50$°C$ for 48 hours. The film casting solution had the following composition (weight%):

aromatic polyamide	16.91
lithium nitrate	6.93
dimethyl acetamide(DMA)	76.16

The polymer powder was put into a glass container containing lithium nitrate and the solvent dimethyl acetamide for three days for the polymer to be fully dissolved. The polymer solution was light yellow, semitransparent and very viscous when polymer was dissolved. This casting solution was filtered and degassed and left overnight after degassing.

The film was cast , by using the casting solution, on a Pyrex glass plate with 0.025 cm (0.01 inch) side runners to give this thickness to the as-cast film. Uniformity of film thickness was also obtained by passing a thick glass rod across the top of the plate, the glass rod resting on the side runners

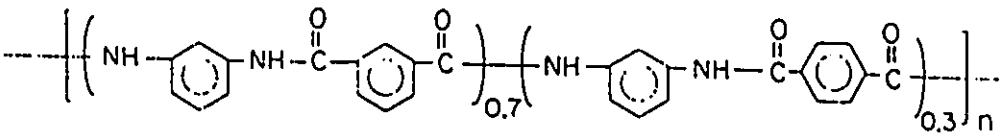

Figure 6: The structure of the repeat unit of poly-m-phenylene-iso(70)-co-tere(30)-phthalamide polymer (aromatic polyamide)[49].

only.

The evaporation time is controlled to be less than five seconds at room temperature of about 23-25°C , after which period, the glass plate with as-cast film on was quickly moved into an oven at 95°C with fan ventilation inside where it was held for 10 minutes. The glass plate containing the partially hardened film was then carefully immersed into ice cold water in a tray where it was left at that temperature overnight. On standing in ice cold water overnight, the film peeled itself off, or could be removed by hand easily, from the surface of the glass plate. The film was cut into small round coupon-like membranes. There was no heat treatment applied to PA membrane. The pressurization procedures were conducted the same way as that for CAB membranes which was descibed earlier in this chapter. The PA membranes were stored in a 3 wt.% ethyl alcohol water solution.

4.2 Description of Reverse Osmosis Experiments

4.2.1 Reverse Osmosis Apparatus

The static reverse osmosis cell, which is used in the experiments, illustrated in Fig.7 & 8 is a stainless steel pressure chamber consisting of two detachable parts. The membrane is mounted on a stainless steel porous plate embedded in the lower part of the cell through which the membrane permeated liquid is withdrawn at atmospheric pressure. The upper part of the cell contains the feed solution under pressure which is in contact with the membrane. The two parts of the cell are clamped and sealed tight using rubber O-rings. Compressed nitrogen gas was used to pressurize the system. About 200 cc.. of feed solution is used each time. The feed solution

is kept stirred during the experiment by means of a magnetic stirrer fitted in the cell about one quarter of an inch above the membrane surface.

4.2.2 Testing Procedures

After membranes were installed in static cells and pressurized by compressed nitrogen gas at 5517 kPag (800 psig) for two hours, the pure water permeation rate was measured with distilled water at 1724 kPag (250 psig) by collecting samples after 2 hours running, weighing the sample collected for a set period of time, usually 15 minutes. Afterwards, 250 cc. of 3500 ppm NaCl aqueous solution was fed into the cell and 1724 kPag (250 psig) pressure was applied. The first 5 mL of membrane permeated solution, which was referred as product, was discarded and the next 5 mL of product was collected as a sample in a weighed dry glass bottle. The time consumed to accumulate 5 mL of product was recorded. The product rate was calculated by dividing the weight of the product by the time taken. In all the cases, the pure water permeability and product rate were reported in units of g/h for 9.6 cm^2 effective membrane surface area at 1724 kPag (250 psig).

In each experiment , the NaCl rejection rate, f, was calculated by

$$f = \frac{feed\ concentration - product\ concentration}{feed\ concentration} \tag{37}$$

where the concentrations of feed and product were determined by specific resistance measurements using a conductivity meter (Model CDM80, Bach-Simpson Ltd.). In all the sample analysis, the very first 5 mL of the product was always discarded and the next 5 mL of product was collected and analysed. Unless otherwise stated , the experiments were of the short run type, each lasting for about 2 hours. They were carried out at the

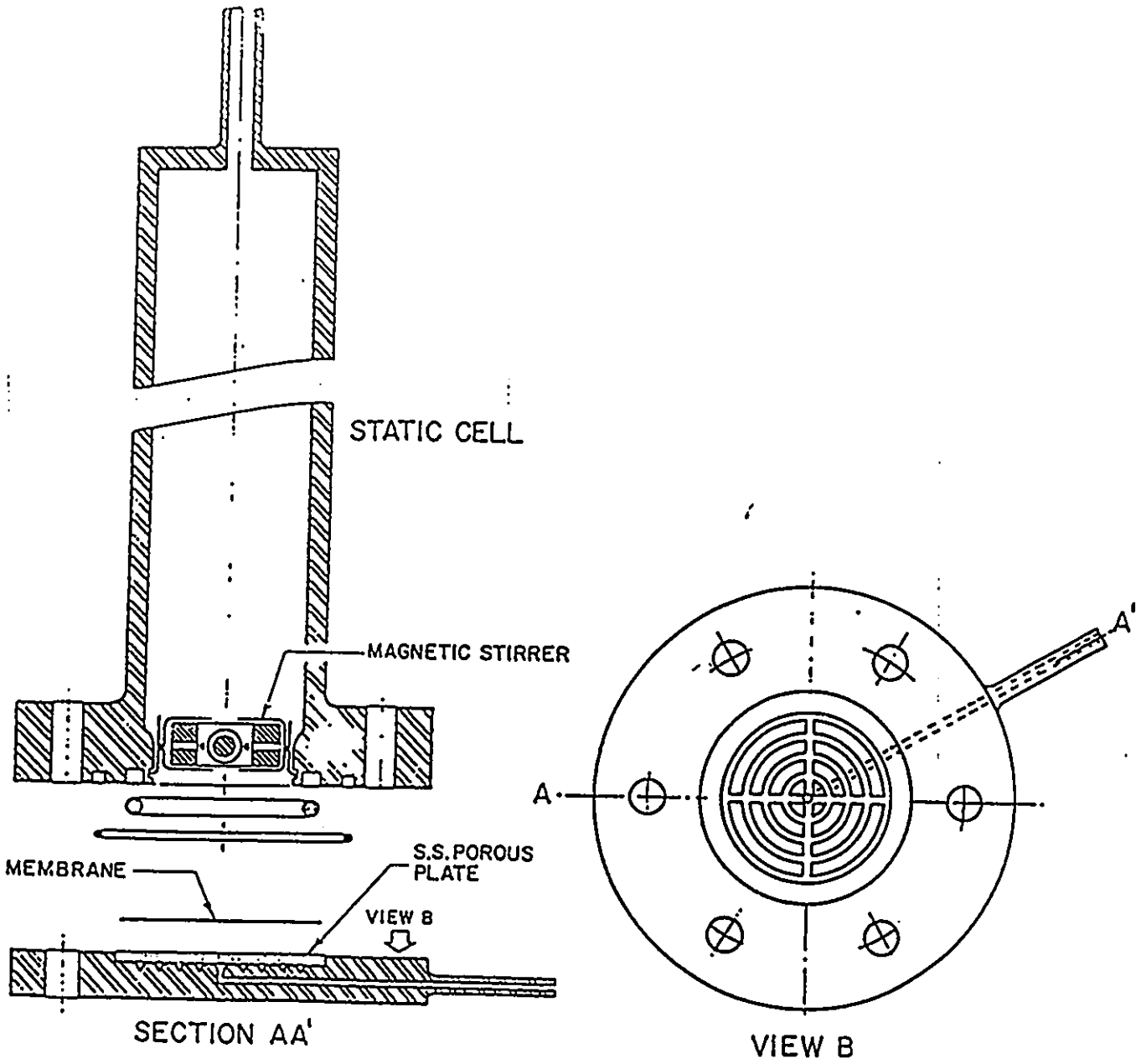

Figure 7: Static cell

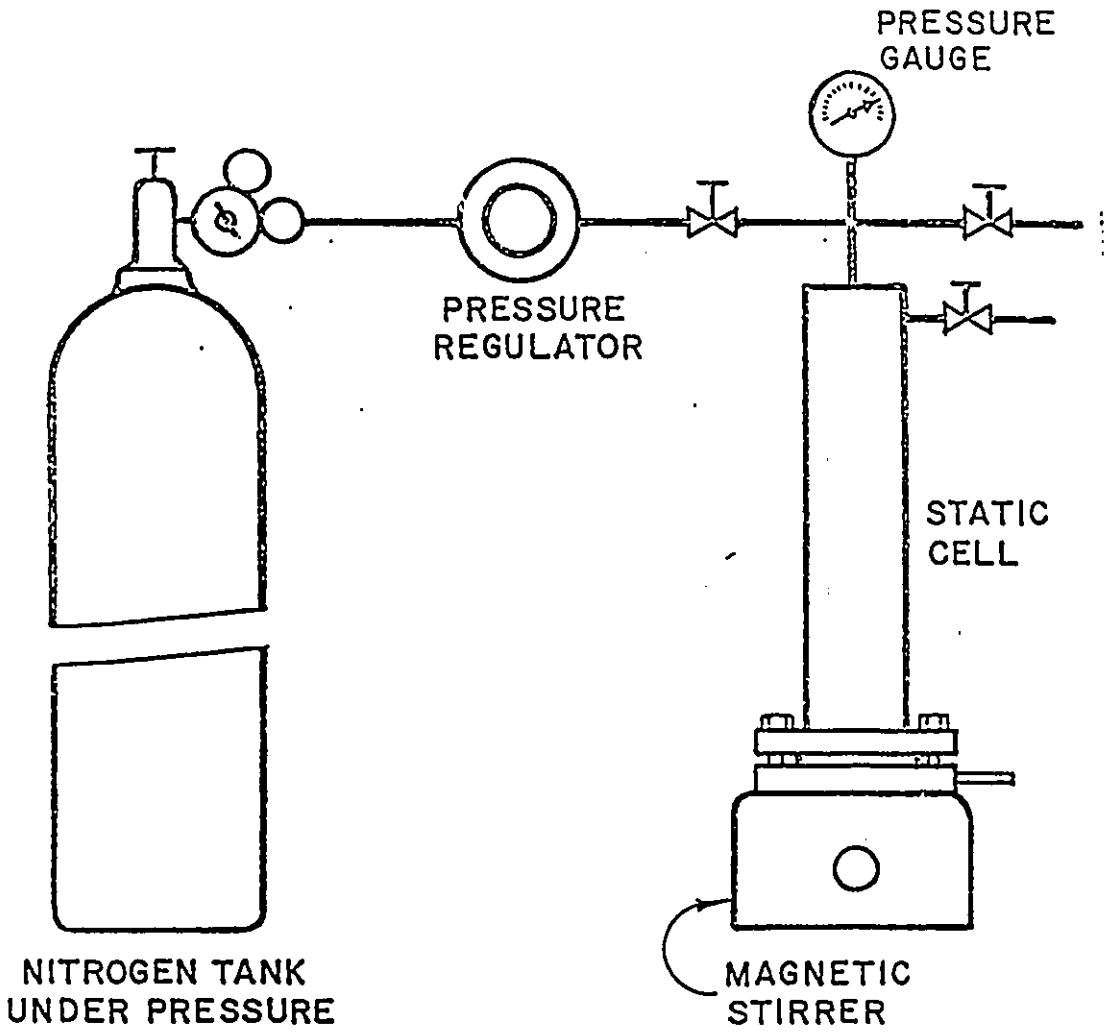

Figure 8: Static cell flow diagram

laboratory temperature (23-25°C).

The shift from aqueous system to nonaqueous one was described as follows. First, the above cell was washed with 250 cc. distilled water for three times. Second, the membrane was fed with a 25wt.%, 50wt.%, 75wt.% and 100wt.% ethyl alcohol aqueous solution under the pressure of 1724 kPag (250 psig), successively for two hours. Third, 250 cc of pure solvent (either constituent of a chosen binary organic mixture) was fed into the cell under 1724 kPag (250 psig) for 2 hours. Fourth, 5 mL of the membrane permeated product was collected in a weighed glass bottle. Pure solvent permeation rate was determined by the weight difference of the sampling bottle divided by the time taken, usually 30-60 minutes, to collect the sample. Fifth, 250 cc. of binary mixture was fed in each run. 5 mL of membrane permeated product was collected after the initial 3 mL membrane permeated product was discarded. The product rate was also determined by dividing the sample weight by the time taken with respect to the same effective membrane area mentioned above.

Analysis of binary mixture composition was done by refractometry. A Waters Differential Refractometer R401 was used. A gas chromatography, Varian Aerograph Series 1400, was occasionally used. Each time, 10 μL of sample was injected. HPLC grade ethyl alcohol was used as carrier solvent. The flow rate of the carrier solvent was set at 1.0 mL/min. A column with 0.8893 g cellulose acetate was connected between the injector tubing and the refractometer detector to generate smooth, reproducible response signal from the refractometer.

4.2.3 Model Systems

Four organic liquid mixtures had been chosen as model systems and tested throughout this study. They were chosen in view of the need for process development reasons.

These four systems were:

$$Ethyl\ alcohol\ +\ n-heptane$$

$$Ethyl\ alcohol\ +\ p-xylene$$

$$Ethyl\ alcohol\ +\ 1-hexanol$$

$$n-Heptane\ +\ p-xylene$$

They represented the combination of:

$$alcohol\ +\ aliphatic\ hydrocarbon$$

$$alcohol\ +\ aromatic\ hydrocarbon$$

$$alcohol\ 1\ +\ alcohol\ 2$$

$$aliphatic\ hydrocarbon\ +\ aromatic\ hydrocarbon.$$

The other reason for the choice of these combinations was that they were completely miscible with each other within the entire range of concentrations, which allowed easy analysis by a refractometer.

4.3 Liquid Chromatography Experiments

4.3.1 Column Packing

A stainless steel pipe with length of 0.6096 meters (two feet) and inside diameter of 0.001575 meters (0.062 inches) was packed with the polymer powder from which the membrane was made. Cellulose acetate butyrate purchased from Eastman Kodak was fine powder. Aromatic polyamide powder was obtained by crushing the PA repeatedly in a mill machine

(Thomas-Wiley Laboratory Mill, Model 4 from Arthur H.Thomas Company,Philadelphia,PA,U.S.A.) in the Department of Chemical Engineering at the University of Ottawa till the powder was fine enough. The powder was dried at $60°C$ overnight. The particle size for the column was kept in the range 38-53 μm by sieving for both CAB and PA materials. The polymer powder was packed dry under the vacumn. The column was weighed before and after packing. 0.5120 g CAB and 0.7960 g PA were packed in two separate columns. The column was washed by pure ethyl alcohol continuously overnight and then it was tested in the system.

4.3.2 Liquid Chromatography Apparatus and Experimental Details

A Waters Associate Liquid Chromatograph (Model 501) fitted with a R401 refractometer was used in this work. The refractometer signal was fed to a Waters 745 integrator. The time taken for the appearance of a maximum recorded response after each injection was defined as the retention time. The system setup is given in Figure 9.

To conduct the experiment, a mixture of solvent A and solvent B of known composition was pumped into the column as a chromatography solvent. Then 10 μL of pure A and 10 μL of pure B were manually injected from a 50 μL Hamilton syringe into the solvent stream as chromatography samples and retention times $[V_R']_A^{mixt}$ and $[V_R']_B^{mixt}$ were recorded corresponding to the given solution compositon. The mobile phase flow rate was set at 0.3 mL/min and the column pressure drop was less than 300 psig. A 15 micron filter was used in between the column outlet and the detector inlet.

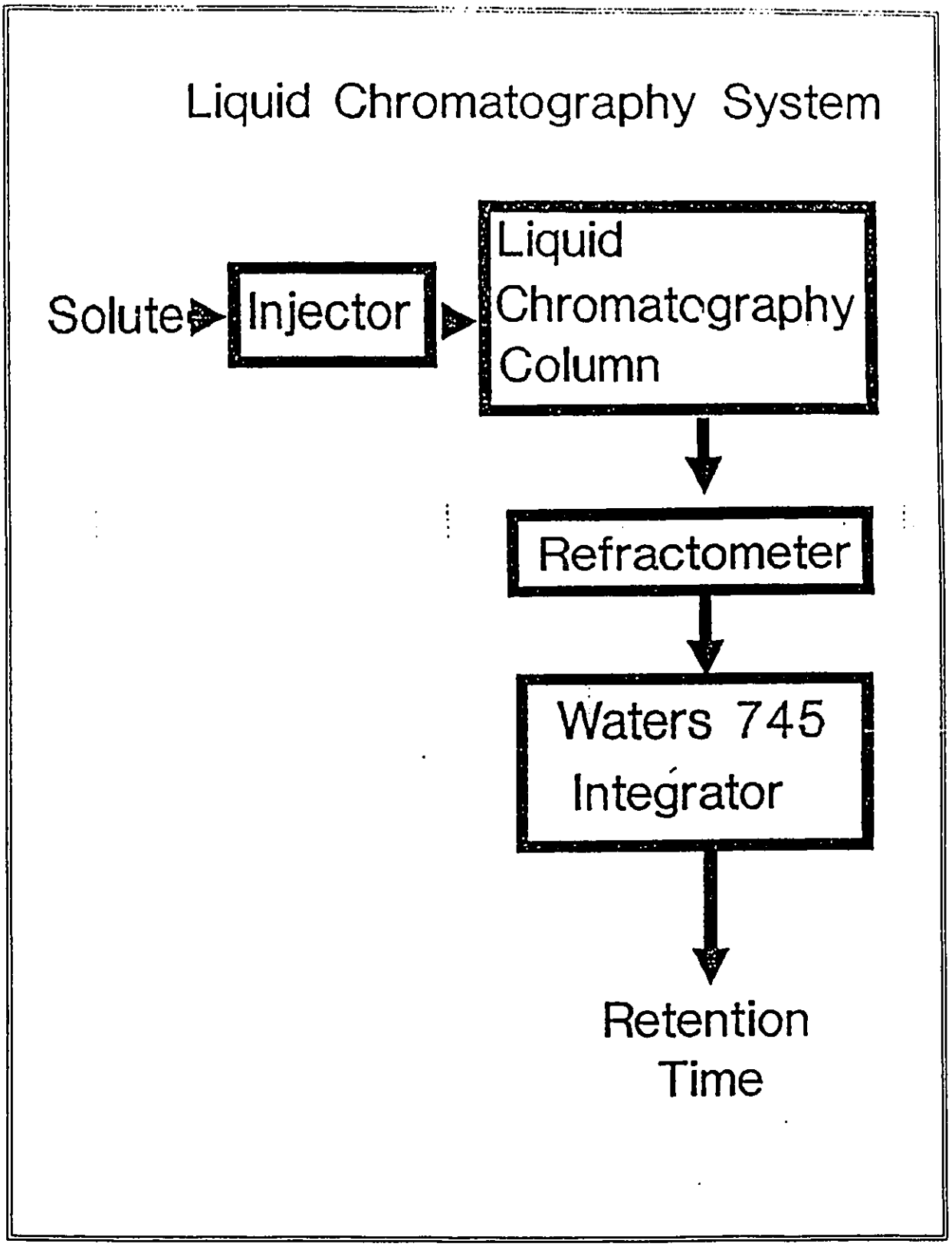

Figure 9: Liquid chromatography system set-up.

This filter was kept in a 50 wt.% nitric acid aqueous solution after use every day. Surface excess values were calculated from the experimental retention time data from equation 35. Thus the surface excess was obtained in the entire composition range of the binary mixture.

Chapter 5

5 Results

5.1 CAB Membrane Shrinkage Studies

Cellulose acetate butyrate membranes were shrunk in distilled hot water. An appropriate shrinkage temperature was determined from the experimental data in Table 2 and the corresponding Figure 10.

Table 2: CAB membrane shrinkage temperature studies

Shrinkage temperature$^{\circ}C$	NaCl separation rate %*	Flux, g/h**
not shrunk	96.6	3.10
60	94.7	2.72
70	97.1	2.53
80	95.4	1.94
90	97.6	1.45
96	98.0	1.10

* 3500 ppm NaCl aqueous feed solution under 1724 kPag (250 psig).

** Based on the effective membrane area of 9.6 cm^2.

The membrane shrunk at 70$^{\circ}C$ exhibited a high NaCl separation rate and reasonably high flux. Thus 70$^{\circ}C$ was chosen as an appropriate shrinkage temperature which was used throughout the CAB membrane preparation.

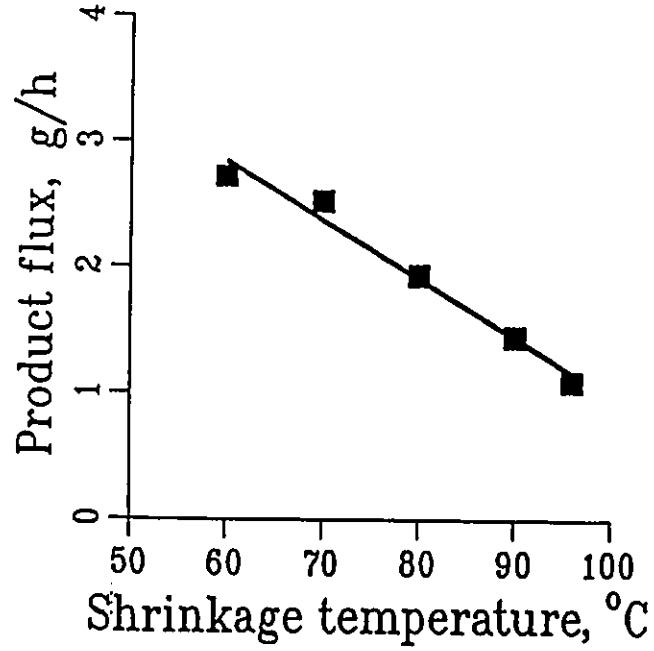

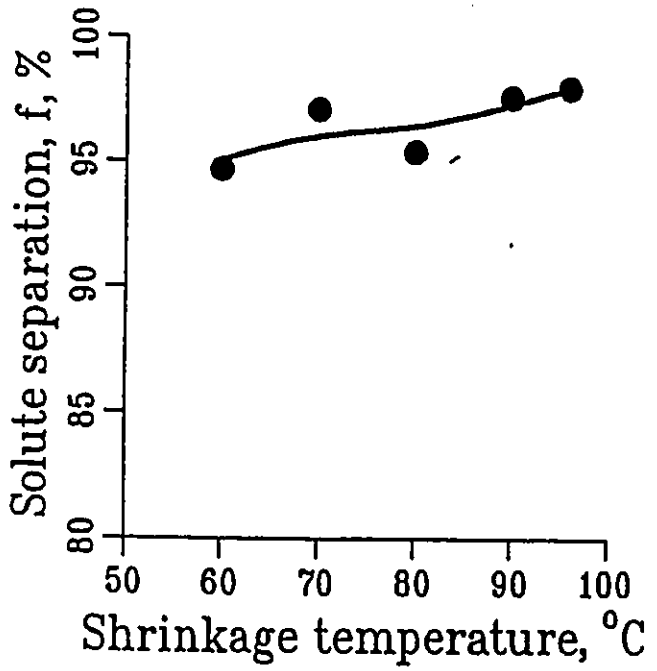

Figure 10: Effect of shrinkage temperature on cellulose acetate butyrate membrane performance corresponding to performance data given in Table 2. RO testing conditions: 3500 ppm NaCl-water feed solution, operating pressure: 1724 kPag (250 psig). Membranes were shrunk with distilled water for ten minutes.

5.2 Results of Reverse Osmosis Experiments

Both cellulose acetate butyrate (CAB) membranes and aromatic polyamide (PA) membranes were first tested with NaCl aqueous solution and then tested in nonaqueous liquid mixtures by following the procedures described in Chapter 4. These testing results were summarized in Table 3 for CAB membranes, and in Table 4 for PA membranes, respectively.

Table 3 RO Separation Data on Organic Liquid Mixtures
I. Data with Cellulose Acetate Butyrate (CAB) Membranes

No.	NaCl Sepn %[a]	Organic Liquid Mixture System A-B	Operating Pressure, psig					
			500			750		
			Mole% A in		Product	Mole% A in		Product
			Feed	Product	Flux[b] g/h	Feed	Product	Flux[b] g/h
1	94.5	Ethyl alcohol -n-Heptane	0.130	0.232	5.08	0.000	0.000	8.41
			0.235	0.338	3.60	0.140	0.315	1.51
			0.375	0.505	2.90	0.375	0.625	3.97
			0.530	0.635	2.82	0.570	0.760	4.31
			0.700	0.740	2.04	0.725	0.870	4.52
			0.885	0.887	2.46	0.900	0.900	4.97
						1.000	1.000	5.09
2	82.9	Ethyl alcohol -n-Heptane	0.000	0.000	11.24	0.000	0.000	4.71
			0.080	0.380	2.87	0.115	0.380	3.21
			0.380	0.620	3.12	0.330	0.600	2.93
			0.510	0.748	3.14	0.500	0.732	3.31
			0.720	0.850	3.15	0.700	0.830	3.96
			0.902	0.940	3.57	0.900	0.912	3.84
			1.000	1.000	3.39	1.000	1.000	6.29
3	82.9	Ethyl alcohol -p-Xylene	0.000	0.000	3.96	0.000	0.000	6.47
			0.100	0.280	3.53	0.110	0.130	4.81
			0.285	0.520	2.77	0.280	0.380	4.00
			0.515	0.590	2.70	0.510	0.618	3.94
			0.710	0.795	2.86	0.712	0.740	3.76
			0.900	0.920	2.85	0.900	0.903	8.98
			1.000	1.000	6.06	1.000	1.000	15.11
4	96.9	Ethyl alcohol -p-Xylene	0.000	0.000	5.62	0.000	0.000	9.83
			0.100	0.180	4.88	0.070	0.135	6.96
			0.285	0.420	4.25	0.280	0.310	6.06
			0.515	0.625	3.91	0.510	0.555	4.77
			0.710	0.756	3.69	0.712	0.730	5.38
			0.900	0.910	4.23	0.900	0.916	4.56
			1.000	1.000	3.77	1.000	1.000	5.87

Table 3 (continued)

L. Data with Cellulose Acetate Butyrate (CAB) Membranes

No.	NaCl Sepn %[a]	Organic Liquid Mixture System A-B	Operating Pressure, psig: 500 — Mole% A in Feed	500 — Mole% A in Product	500 — Product Flux[b] g/h	750 — Mole% A in Feed	750 — Mole% A in Product	750 — Product Flux[b] g/h
5	70.2	Ehtyl alcohol -1-Hexanol	0.000	0.000	3.67	0.000	0.000	0.80
			0.140	0.380	4.20	0.100	0.280	0.95
			0.300	0.330	6.15	0.325	0.495	1.28
			0.500	0.550	6.44	0.530	0.622	1.70
			0.691	0.695	8.09	0.710	0.743	2.41
			0.902	0.910	13.21	0.898	0.904	3.80
			1.000	1.000	15.04	1.000	1.000	4.49
6	85.3	Ethyl alcohol -1-Hexanol	0.000	0.000	21.22	0.000	0.000	2.59
			0.140	0.210	26.42	0.100	0.150	3.02
			0.300	0.378	38.85	0.325	0.400	4.25
			0.500	0.535	38.38	0.530	0.570	5.35
			0.691	0.730	46.48	0.710	0.725	7.53
			0.902	0.920	77.86	0.898	0.908	12.18
			1.000	1.000	85.10	1.000	1.000	18.40
7	82.9	n-Heptane -p-Xylene	0.000	0.000	1.38	0.000	0.000	2.09
			0.090	0.180	1.14	0.131	0.220	2.47
			0.318	0.435	2.29	0.320	0.395	2.44
			0.476	0.598	3.28	0.490	0.538	2.28
			0.712	0.770	3.46	0.692	0.750	2.76
			0.910	0.912	7.37	0.880	0.908	3.26
			1.000	1.000	8.22	1.000	1.000	2.83
8	96.9	n-Heptane -p-Xylene	0.000	0.000	1.84	0.000	0.000	2.76
			0.090	0.160	1.86	0.131	0.230	3.32
			0.318	0.420	1.79	0.320	0.345	3.19
			0.476	0.530	1.62	0.490	0.502	3.22
			0.712	0.729	1.15	0.692	0.706	3.72
			0.910	0.912	2.35	0.880	0.890	5.44
			1.000	1.000	3.99	1.000	1.000	4.59

a: 3500 ppm NaCl-water feed, 1724 kPag (250 psig).

b: Effective membrane area: 9.6 cm^2.

Table 4 RO Separation Data on Organic Liquid Mixtures
II. Data with Aromatic Polyamide (PA) Membranes

No.	NaCl Sepn %[a]	Organic Liquid Mixture System A-B	Operating Pressure, psig					
			500			750		
			Mole% A in		Product	Mole% A in		Product
			Feed	Product	Flux[b] g/h	Feed	Product	Flux[b] g/h
9	83.5	Ethyl alcohol -n-Heptane	0.000	0.000	3.82	0.000	0.000	5.02
			0.080	0.250	2.12	0.085	0.100	4.14
			0.200	0.620	2.38	0.270	0.540	3.68
			0.420	0.755	2.32	0.455	0.648	3.52
			0.635	0.830	2.46	0.680	0.850	5.37
			0.870	0.930	2.68	0.880	0.958	6.89
			1.000	1.000	5.01	1.000	1.000	13.44
10	92.9	Ethyl alcohol -n-Heptane				0.000	0.000	2.68
						0.040	0.240	0.99
			0.298	0.825	0.79	0.270	0.727	0.72
			0.498	0.860	1.10	0.395	0.870	0.84
			0.688	0.895	1.80	0.720	0.931	1.20
			0.855	0.928	3.80	0.920	0.978	2.80
			1.000	1.000	11.90	1.000	1.000	3.24
11	83.8	Ethyl alcohol -p-Xylene	0.000	0.000	0.46	0.000	0.000	0.54
			0.150	0.448	0.25	0.095	0.168	0.79
			0.365	0.617	0.83	0.385	0.590	1.14
			0.470	0.702	0.78	0.525	0.720	1.38
			0.710	0.848	1.10	0.720	0.832	2.24
			0.902	0.938	1.79	0.906	0.932	3.27
			1.000	1.000	2.74	1.000	1.000	3.70
12	96.2	Ethyl alcohol -p-Xylene	0.150	0.441	0.55	0.095	0.218	0.29
			0.365	0.650	0.48	0.385	0.591	0.91
			0.470	0.732	0.49	0.525	0.712	1.13
			0.710	0.830	0.79	0.700	0.860	2.34
			0.902	0.951	1.91	0.906	0.938	3.09
			1.000	1.000	4.14	1.000	1.000	4.30

Table 4 (continued)

II. Data with Aromatic Polyamide (PA) Membranes

No.	NaCl Sepn %[a]	Organic Liquid Mixture System A-B	Operating Pressure, psig					
			500			750		
			Mole% A in		Product	Mole% A in		Product
			Feed	Product	Flux[b] g/h	Feed	Product	Flux[b] g/h
13	83.8	Ethyl alcohol -1-Hexanol	0.540	0.660	0.30	0.090	0.180	0.03
			0.690	0.818	0.76	0.305	0.550	0.13
			0.890	0.910	1.67	0.540	0.705	0.48
			1.000	1.000	4.88	0.693	0.855	0.68
						0.880	0.903	2.52
						1.000	1.000	2.92
14	96.0	Ethyl alcohol -1-Hexanol	0.000	0.000	0.23	0.000	0.000	0.18
			0.090	0.310	0.28	0.090	0.305	0.23
			0.320	0.490	0.49	0.305	0.790	1.02
			0.540	0.610	0.34	0.540	0.603	0.92
			0.690	0.742	0.86	0.693	0.760	1.71
			0.890	0.908	2.02	0.903	0.920	3.36
			1.000	1.000	5.40	1.000	1.000	5.84
15	95.7	n-Heptane -p-Xylene	0.300	0.490	0.67	0.000	0.000	0.30
			0.445	0.635	0.48	0.102	0.410	0.48
			0.701	0.792	3.36	0.396	0.480	1.13
			0.910	0.921	8.91	0.540	0.580	1.71
			1.000	1.000	5.99	0.700	0.760	4.07
						0.890	0.906	4.80
						1.000	1.000	9.19

a: 3500 ppm NaCl-water feed, 1724 kPag (250 psig).

b: Effective membrane area: 9.6 cm^2.

5.3 Results of Liquid Chromatography Experiments

Experimental retention time data are shown in Table 5 - 12 for CAB and aromatic polyamide materials for various mixtures of organic liquids. The surface excess data calculated on the basis of experimental retention time data are also shown. The method of calculation was described in Chapter 3. The variance for each solute retention time indicated by the relative error percentage was controlled below 2.0% level. The relative error percentage was calculated by the formula:

$$relative\ error\ \% = \frac{individual\ retention\ time - average\ retention\ time}{average\ retention\ time} \tag{38}$$

Comparing the experimental retention time data, the following is the increasing order of the retention time for both cellulose acetate butyrate and aromatic polyamide materials:

$p - xylene < ethanol < n - heptane.$

Figure 11-18 are the graphical presentation of the surface excess versus the composition of the liquid mixtures.

Table 5: Retention time data and surface excess for CAB-EtOH-p-xylene

X_A mol%	T_A(EtOH) minutes	T_B(p-xylene) minutes	Surface Excess $\Gamma_A A_p V_A$, cm^3
1.0	/////	/////	0
0.9	6.610	5.220	6.419 E-02
0.8	6.657	5.070	10.770 E-02
0.7	6.627	4.957	12.490 E-02
0.6	6.627	4.953	12.190 E-02
0.5	6.353	4.910	9.440 E-02
0.4	6.670	5.177	8.169 E-02
0.3	6.493	5.517	4.107 E-02
0.2	6.733	5.993	2.101 E-02
0.1	7.500	6.990	0.727 E-02
0.0	/////	/////	0

column: CAB171-40 0.5120 g CAB

T_A, T_B == retention time of EtOH, p-xylene, resp.
X_A == mole fraction of EtOH
solvent flowrate: 0.3 mL/min
injection volume: 10 µL

Table 6: Retention time data and surface excess for CAB-EtOH-1-hexanol

X_A mol%	T_A(EtOH) minutes	T_B(1-hexanol) minutes	Surface Excess $\Gamma_A A_b V_A$, cm^3
1.0	/////	/////	0
0.9	6.100	5.700	1.8591 E-02
0.8	6.250	5.920	2.2459 E-02
0.7	6.280	6.235	3.3683 E-02
0.6	6.320	6.380	-0.4363 E-02
0.5	6.390	6.365	0.1630 E-02
0.4	6.380	6.275	0.5714 E-02
0.3	6.460	6.255	0.8566 E-02
0.2	6.430	6.230	0.5632 E-02
0.1	6.535	6.300	0.3317 E-02
0.0	/////	/////	0

column: CAB171-40 0.5120 g CAB

T_A, T_B == retention time of EtOH and 1-hexanol, resp.
X_A == mole fraction of EtOH
solvent flow rate: 0.3 mL/min
injection volume: 10 µL

Table 7: Retention time data and surface excess for CAB-n-heptane-p-xylene

X_A mol%	T_A(p-xylene) minutes	T_B(n-heptane) minutes	Surface Excess $\Gamma_A A_B V_A$, cm^3
1.0	/////	/////	0
0.9	5.089	6.352	-3.903 E-02
0.8	4.975	6.175	-6.356 E-02
0.7	4.470	5.555	-7.243 E-02
0.6	4.530	5.600	-7.917 E-02
0.5	4.334	5.430	-8.159 E-02
0.4	4.266	5.556	-8.910 E-02
0.3	4.308	5.655	-7.873 E-02
0.2	5.434	6.234	-3.447 E-02
0.1	5.100	6.389	-3.024 E-02
0.0	/////	/////	0

column: CAB171-40 0.5120 g CAB

T_A, T_B == retention time p-xylene and n-hetane, resp.
X_A == mole fraction of p-xylene
solvent flow rate: 0.3 mL/min
injection volume: 10 µL

Table 8: Retention time data and surface excess for CAB-EtOH-n-heptane

X_A mol%	T_A(EtOH) minutes	T_B(n-Heptane) minutes	Surface Excess $\Gamma_A A_p V_A$, cm^3
1.0	/////	/////	0
0.9	4.850	6.703	-9.4766 E-02
0.8	4.833	6.345	-10.7449 E-02
0.7	4.567	6.163	-11.9544 E-02
0.6	4.707	6.047	-9.4136 E-02
0.5	4.933	6.247	-8.0328 E-02
0.4	4.997	6.233	-6.1503 E-02
0.3	4.943	6.493	-5.7946 E-02
0.2	5.057	6.677	-4.0050 E-02
0.1	5.620	7.443	-2.2210 E-02
0.0	/////	/////	0

column: CAB 171-40 0.5120 g CAB

T_A, T_B == retention time of EtOH, n-heptane, resp.
X_A == mole fraction of EtOH
solvent flowrate: 0.3 mL/min
injection volume: 10 µL

Table 9: Retention time data and surface excess for PA-EtOH-p-xylene

X_A mol%	T_A(EtOH) minutes	T_B(p-xylene) minutes	Surface Excess $\Gamma_A A_p V_A$, cm^3
1.0	/////	/////	0
0.9	8.255	7.225	4.7562 E-02
0.8	9.310	8.015	8.7853 E-02
0.7	8.265	7.130	8.4913 E-02
0.6	8.215	7.164	7.6564 E-02
0.5	8.210	7.090	7.3279 E-02
0.4	8.345	7.240	6.0458 E-02
0.3	8.335	7.440	3.7657 E-02
0.2	8.340	7.680	1.8741 E-02
0.1	8.515	8.000	0.7337 E-02
0.0	/////	/////	0

column: Aromatic polyamide(PA) 0.7960 g PA

T_A, T_B == retention time of EtOH and p-xylene, resp.
X_A == mole fraction of EtOH.
solvent flowrate: 0.3 mL/min
injection volume: 10 µL

Table 10: Retention time data and surface excess for PA-EtOH-1-hexanol

X_A mol%	T_A(minutes) minutes	T_n(1-hexanol) minutes	Surface Excess $\Gamma_A A_p V_A$, cm^3
1.0	/////	/////	0
0.9	8.135	7.790	16.035 E-03
0.8	8.145	8.005	9.528 E-03
0.7	8.175	8.150	1.871 E-03
0.6	8.170	8.230	-4.363 E-03
0.5	8.170	8.400	-14.992 E-03
0.4	8.205	8.350	-7.890 E-03
0.3	8.255	8.350	-3.969 E-03
0.2	8.365	8.445	-2.253 E-03
0.1	8.490	8.590	-1.411 E-03
0.0	/////	/////	0

column: Aromatic polyamide(PA) 0.7960 g PA

T_A, T_n == retention time of EtOH and 1-hexanol, resp.
X_A == mole fraction of EtOH.
solvent flowrate: 0.3 mL/min
injection volume: 10 µL

Table 11: Retention time data and surface excess for PA-n-heptane-p-xylene

X_A mol%	T_A(p-xylene) minutes	T_B(n-heptane) minutes	Surface Excess $\Gamma_A A_b V_A$, cm^3
1.0	/////	/////	0
0.9	7.465	8.065	-1.8543 E-02
0.8	7.360	8.090	-3.8667 E-02
0.7	7.330	8.075	-4.9965 E-02
0.6	7.225	8.125	-6.6591 E-02
0.5	7.030	8.155	-8.3751 E-02
0.4	7.175	8.110	-6.4583 E-02
0.3	7.200	8.250	-6.1368 E-02
0.2	7.310	8.385	-4.6317 E-02
0.1	7.560	8.785	-2.8741 E-02
0.0	/////	/////	0

column: Aromatic polyamide(PA) 0.7960 g PA

T_A, T_B == retention time of p-xylene, n-heptane, resp.
X_A == mole fraction of p-xylene.
solvent flow rate: 0.3 mL/min
injection volume: 10 µL

Table 12: Retention time data and surface excess for PA-EtOH-n-heptane

X_A mol%	T_A(EtOH) minutes	T_B(n-heptane) minutes	Surface Excess $\Gamma_A A_B V_A$, cm^3
1.0	/////	/////	0
0.9	7.123	8.460	-6.8377 E-02
0.8	6.825	8.358	-10.8941 E-02
0.7	6.875	8.320	-10.8234 E-02
0.6	6.850	8.080	-8.6409 E-02
0.5	6.825	8.050	-7.4887 E-02
0.4	6.828	8.060	-6.1304 E-02
0.3	6.885	8.080	-4.4674 E-02
0.2	6.975	8.185	-2.9914 E-02
0.1	7.220	8.515	-1.5778 E-02
0.0	/////	/////	0

column: Aromatic Polyamide (PA) 0.7960 g

T_A, T_B == retention time of EtOH and n-heptane, resp.
X_A == mole fraction of EtOH.
solvent flow rate: 0.3 mL/min
injection volume: 10 µL

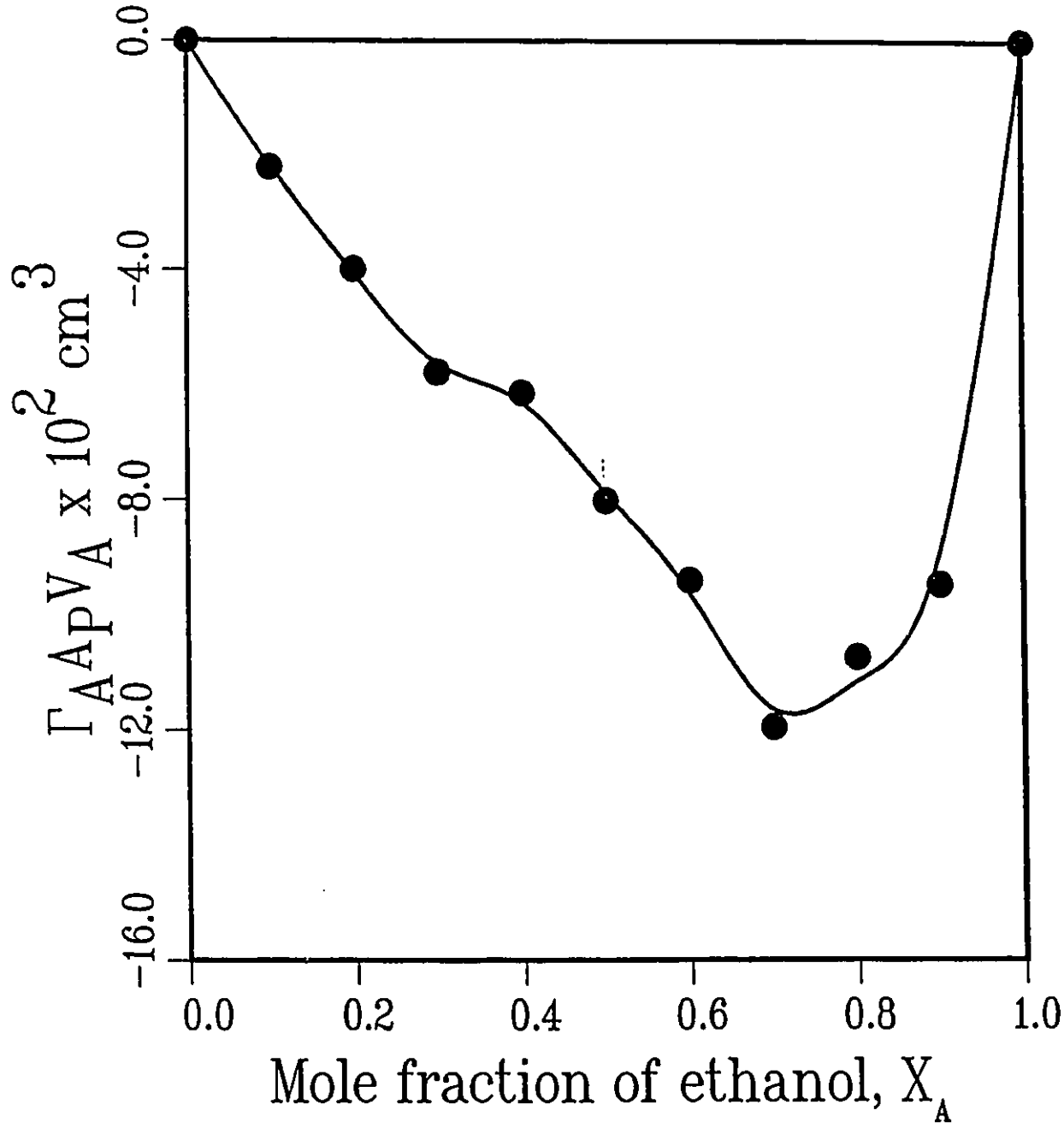

Figure 11: Surface excess for CAB-EtOH-n-heptane.

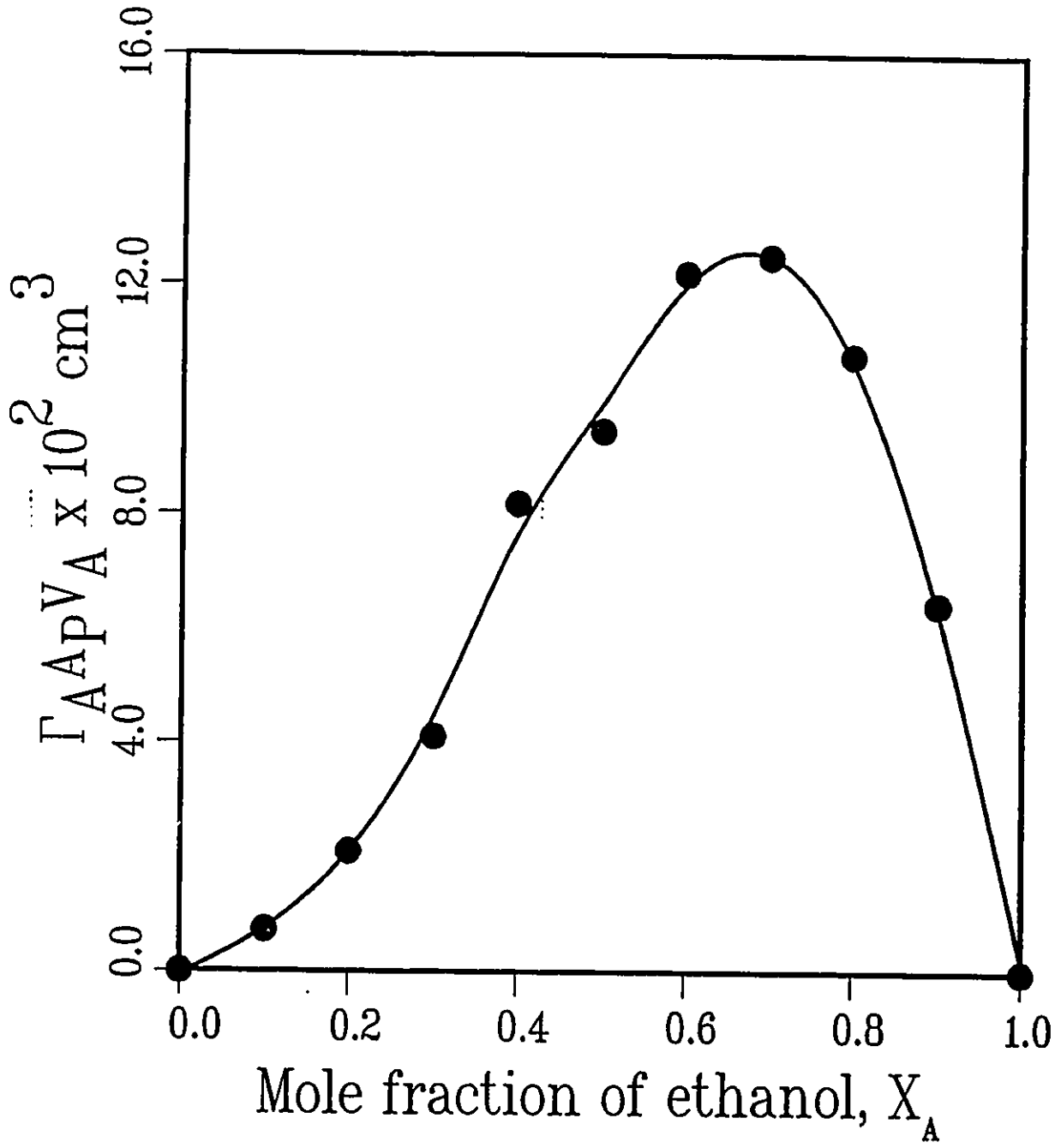

Figure 12: Surface excess for CAB-EtOH-p-xylene.

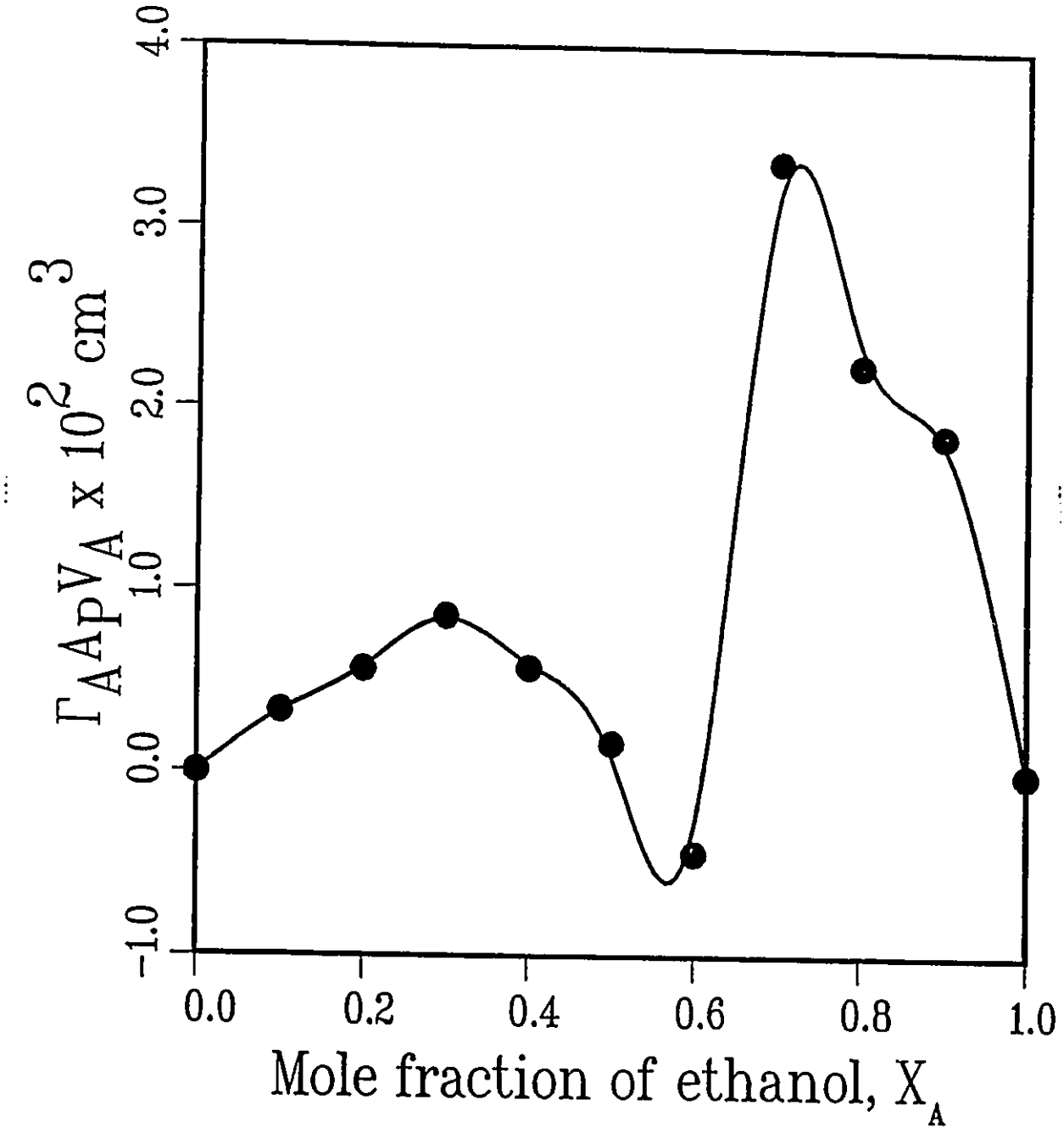

Figure 13: Surface excess for CAB-EtOH-1-hexanol.

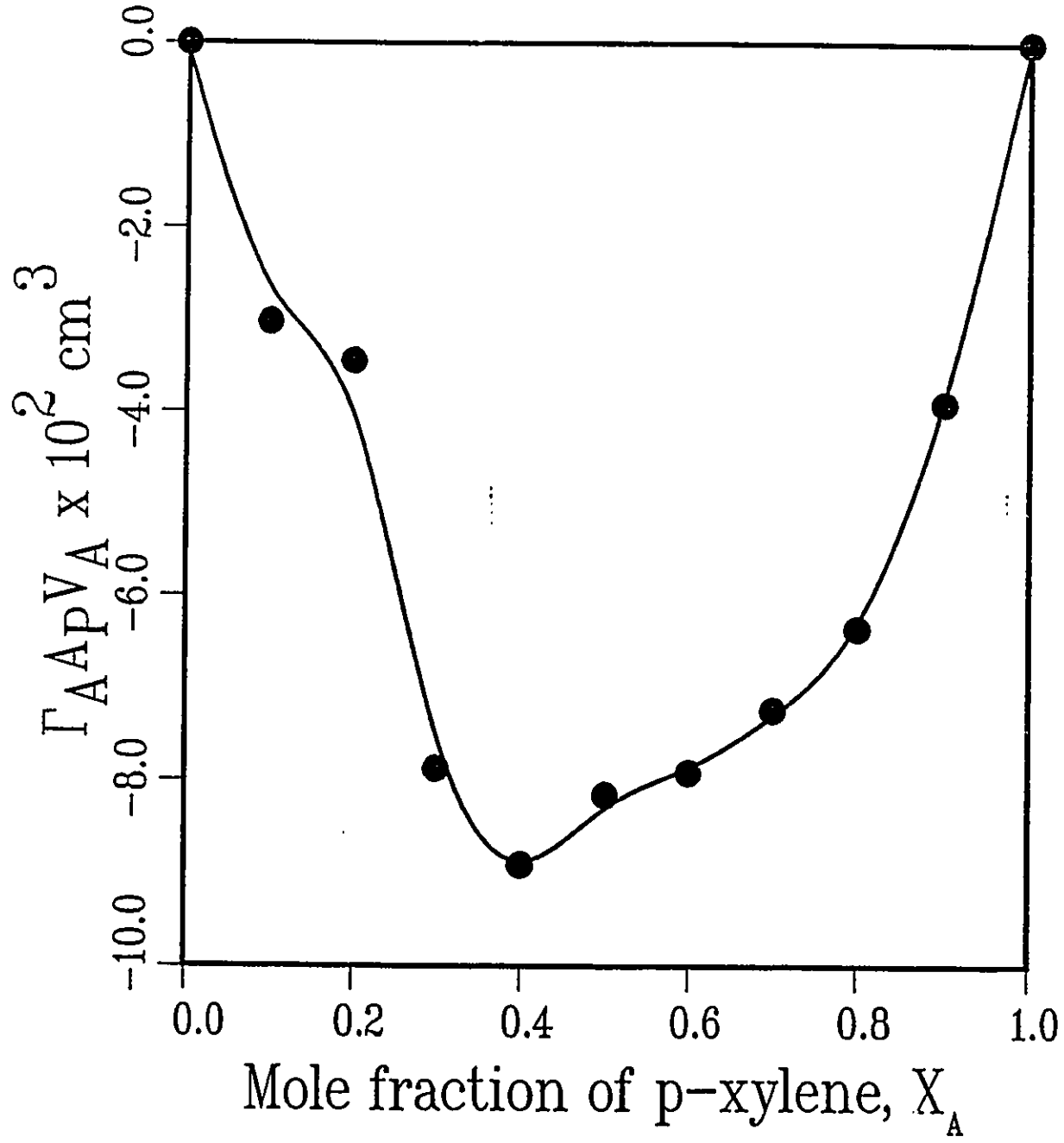

Figure 14: Surface excess for CAB-n-heptane-p-xylene.

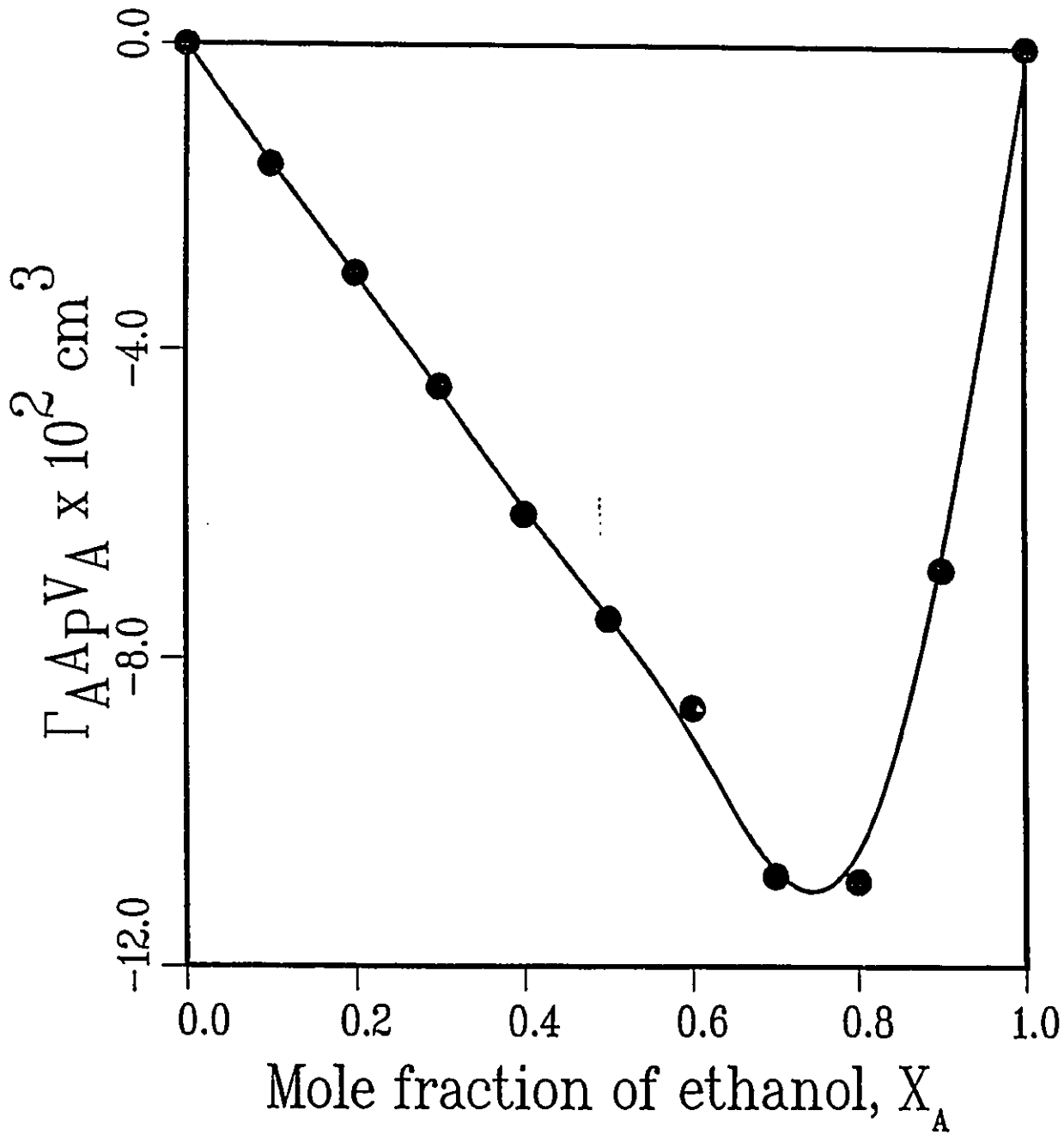

Figure 15: Surface excess for PA-EtOH-n-heptane.

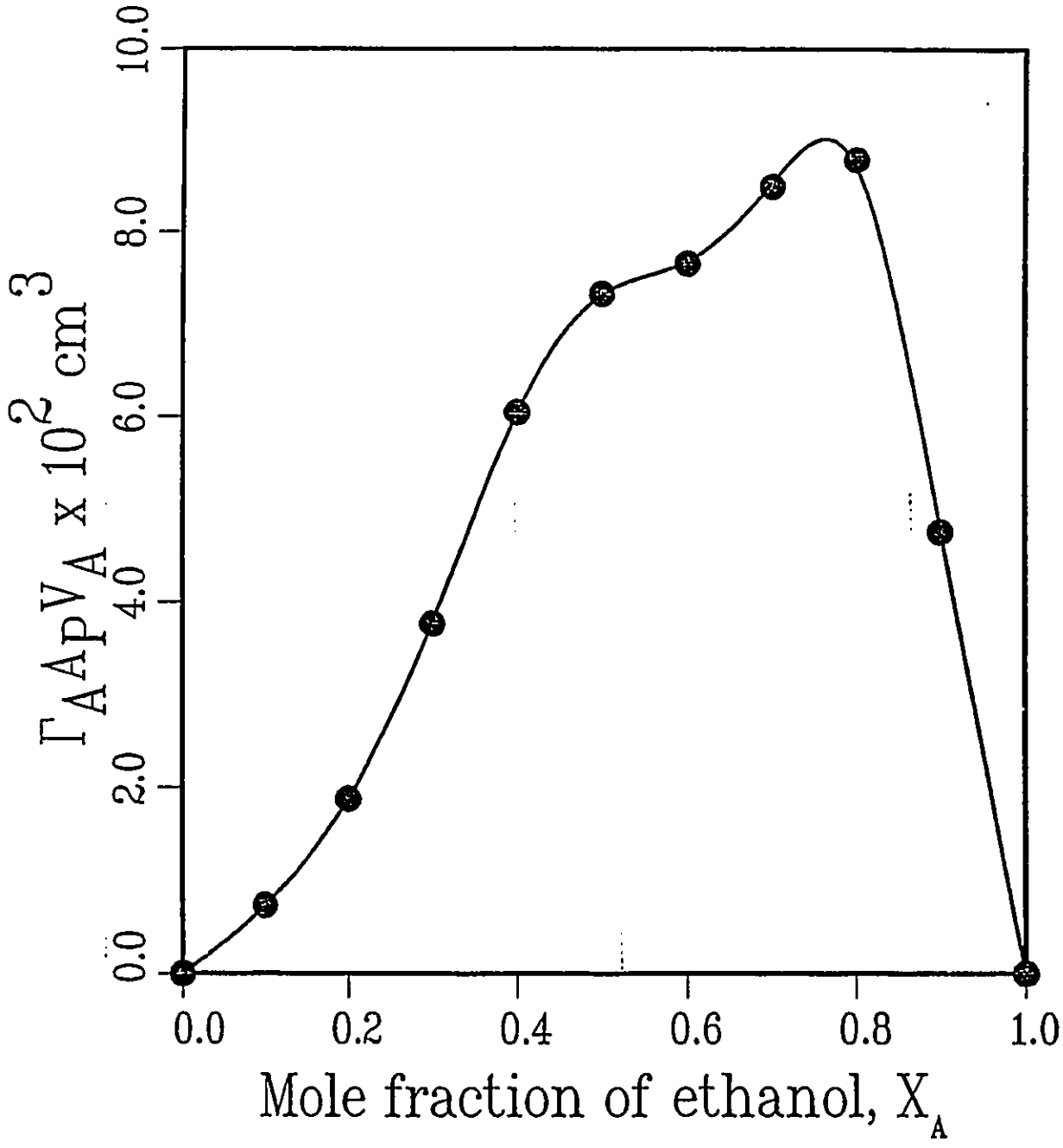

Figure 16: Surface excess for PA-EtOH-p-xylene.

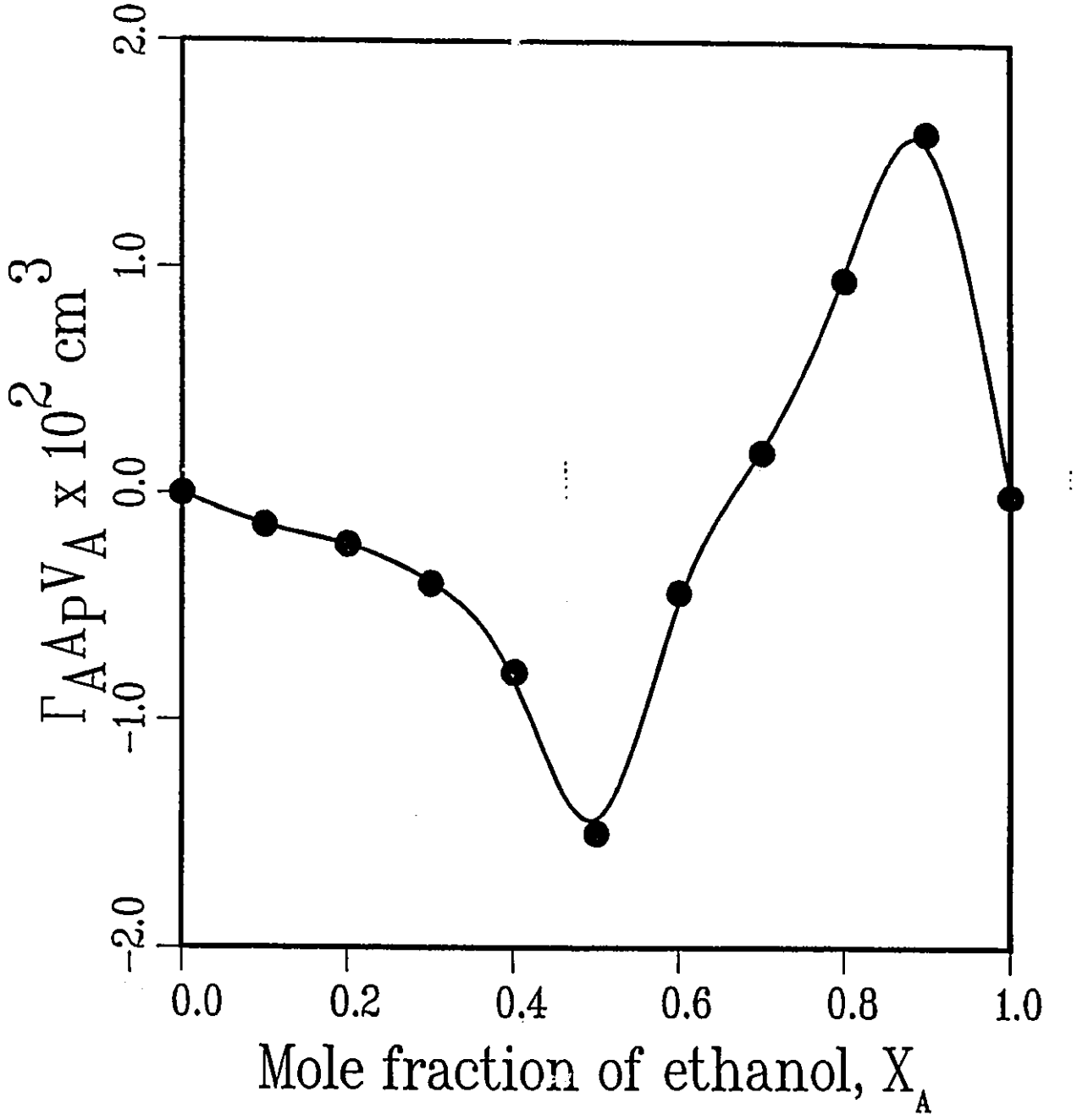

Figure 17: Surface excess for PA-EtOH-1-hexanol.

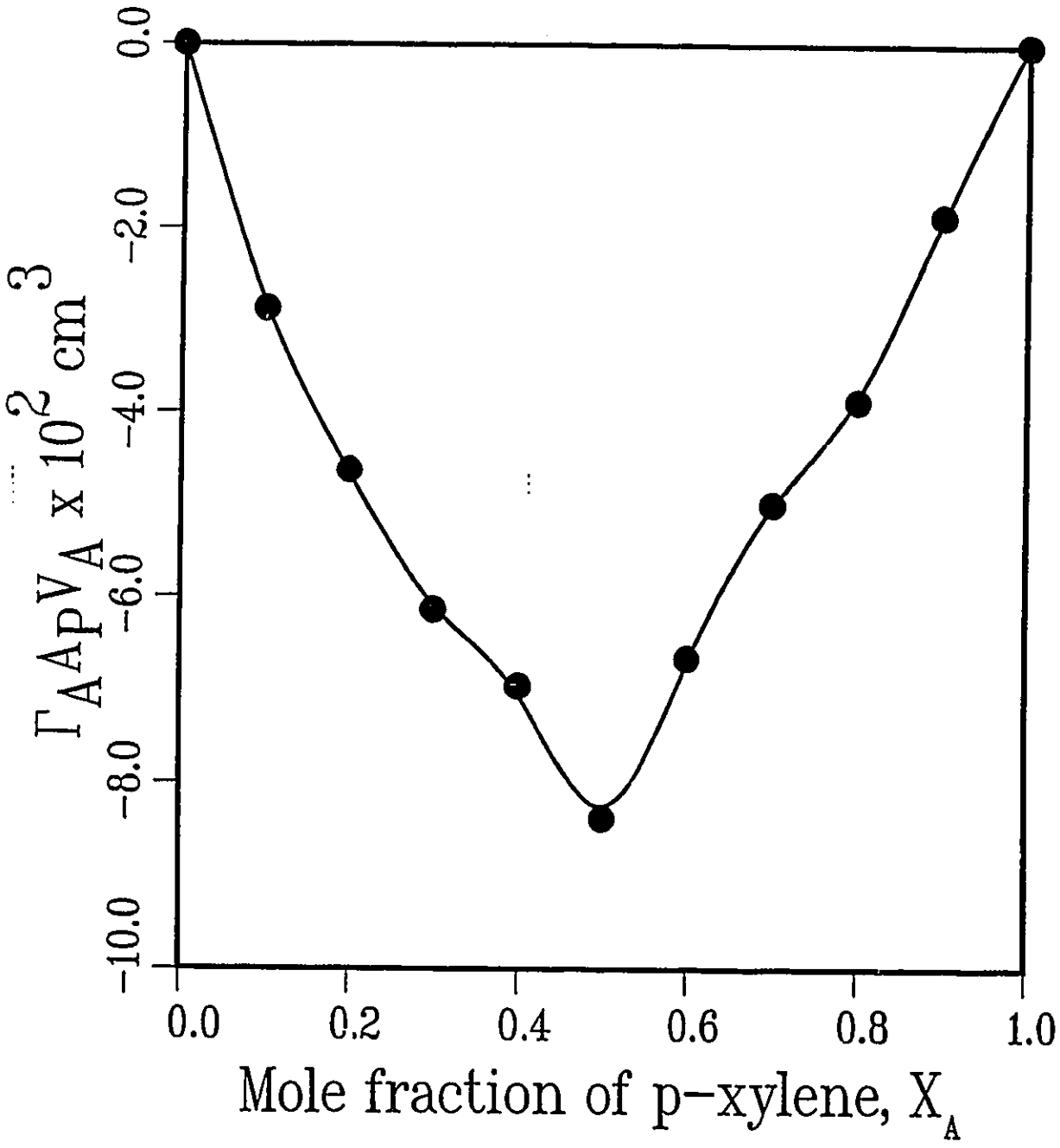

Figure 18: Surface excess for PA-n-heptane-p-xylene.

Chapter 6

6 Discussion

The discussion focuses on three aspects of the experimental data summarized in Chapter 5. The first aspect concerns the reverse osmosis fractionation achieved by CAB and PA membranes, of organic liquid mixtures. The second part of the discussion examines the preferential adsorption of organic liquid components to the polymeric materials, namely CAB and PA. Finally, the membrane separation data are compared with the preferential adsorption data from LC experiments.

6.1 Reverse Osmosis Fractionation of Organic Liquid Mixtures

Table 3 gives the experimental RO fractionation data for the systems ethyl alcohol-n-heptane, ethyl alcohol-p-xylene, ethyl alcohol-1-hexanol, and n-heptane-p-xylene using laboratory prepared cellulose acetate butyrate (CAB) membranes. The results illustrate that separations take place in all the four binary organic liquid mixtures studied, that ethanol is preferentially transported through CAB membrane in the EtOH-n-heptane, the EtOH-p-xylene and the EtOH-1-hexanol feed solution systems whereas n-heptane is preferentially transported through CAB membranes in the n-heptane-p-xylene feed solution system. Referring to Table 4, the above results are also valid when aromatic polyamide (PA) membranes are used.

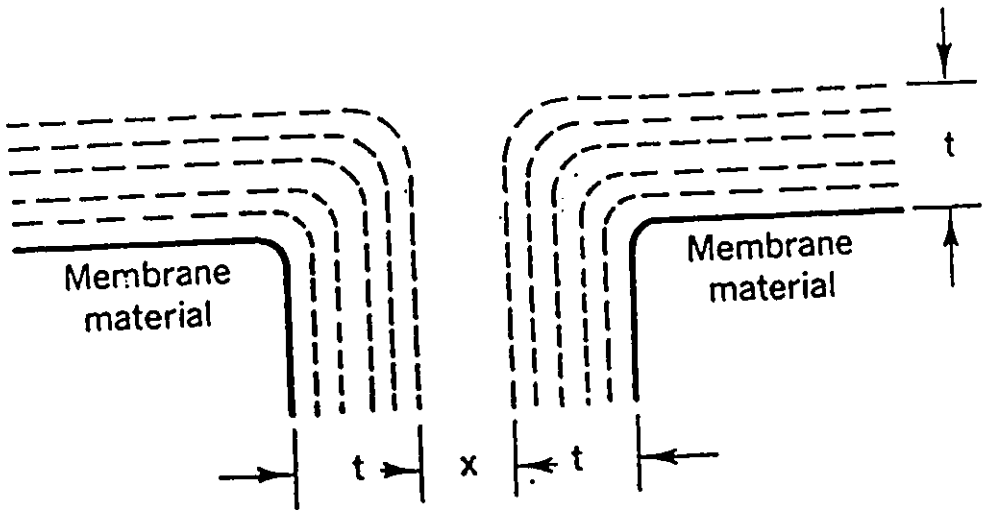

Figure 19: Concept of membrane pore and preferential sorption (t, thickness of interfacial layer; x, thickness of bulk layer) [44].

In order to examine the results in more detail, the effect of operating pressure and average pore size on the membrane surface will be discussed below. An illustration of membrane pore concept is presented in Fig.19.

In the general case, the membrane pore area may be considered to consist of two distinct regions, namely, (i) the 'bulk solution region' in the middle of the pore unaffected by the interfacial forces, (ii) the 'interfacial region' next to the membrane surface including the membrane pore wall.

Effect of operating pressure on the RO fractionation can be divided into three categories. **First** category is represented by the EtOH-n-heptane and the EtOH-1-hexanol feed solution systems as shown in Figure 20 and 21, respectively.

In this category, separation increases with an increase in the operating pressures for both CAB and PA membranes.The above results are understandable on the following basis [45]:

1. The composition of the permeated solution is governed by the relative contribution of the interfacial fluid and the bulk fluid (see Fig.19) to the overall membrane transport. The flow of the bulk fluid does not cause any separation. As for the flow of the interfacial fluid, it results in the enrichment of the preferentially sorbed component in the permeated solution. When by some reasons, the mobility of the interfacial fluid is reduced, the enrichment of the preferentially sorbed component decreases. Further, in the sorbed region, when the mobility of the preferentially sorbed component becomes smaller due to some reasons than that of the non-preferentially sorbed component, the flow of interfacial fluid through the membrane can results in the enrichment of the non-preferentially sorbed component in the

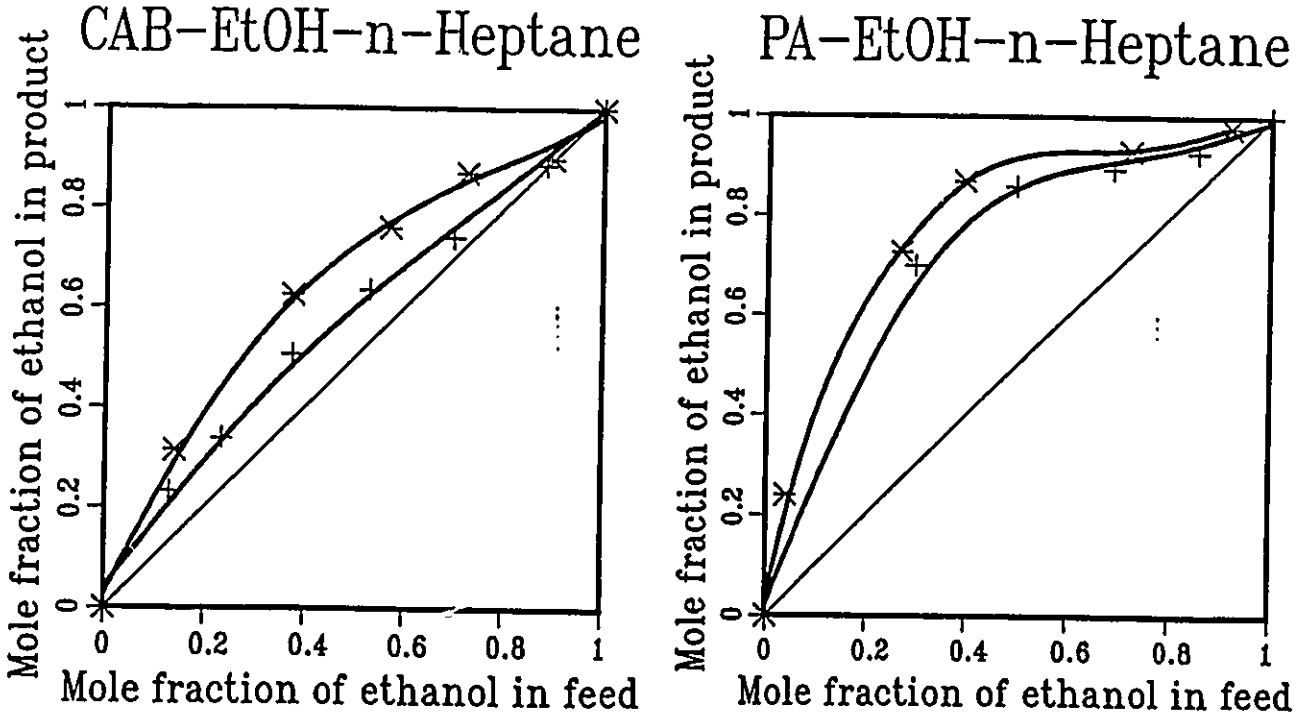

Figure 20: Effect of operating pressure on RO separation for CAB-EtOH-n-heptane and PA-EtOH-n-heptane systems corresponding to RO data given in Table 3,4, film No.1 and 10. Legend for operating pressure: +, 3448 kPag (500 psig); *, 5172 kPag (750 psig).

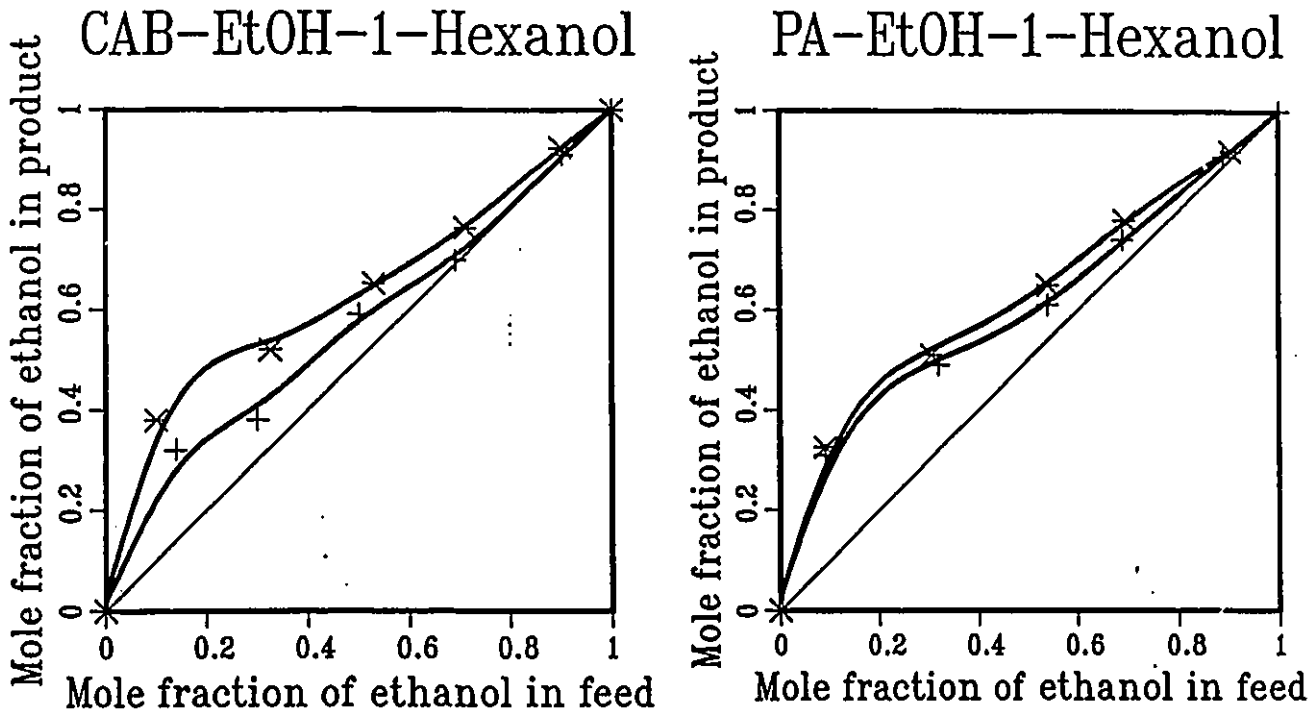

Figure 21: Effect of operating pressure on RO separation for CAB-EtOH-1-hexanol and PA-EtOH-1-hexanol systems corresponding to RO data given in Table 3,4, film No.5 and 14. Legend for operating pressure: +, 3448 kPag (500 psig); *, 5172 kPag (750 psig).

permeate solution.

2. An increase in the operating pressure tends to increase the mobility of the preferentially sorbed layer.

For EtOH-n-heptane system, as determined from the liquid chromatography experiments (see section 6.2, Table 8,12), heptane is the preferentially sorbed component for both CAB and PA materials.

In the sorbed layer, the mobility of ethanol is more than that of heptane as a consequence of the preferential sorption of heptane. Thus, the flow of the interfacial fluid results in the enrichment of the ethanol in the permeate solution. This expectation is consistent with the RO experimental results. When higher operating pressure is applied, the mobility of the preferential sorbed layer increases. Therefore, the enrichment of ethanol is enhanced by the higher operating pressure. Experimental results shown in Fig.20 exhibits this tendency.

For the EtOH-1-hexanol system, as determined from the LC experiments, ethanol is preferentially sorbed for CAB material (see Table 6). Thus, the flow of the interfacial fluid results in the enrichment of ethanol in the permeated solution. An increase in the operating pressure tends to increase more the mobility of the interfacial layer than that of the bulk flow. Therefore, higher operating pressure results in the more enrichment of ethanol in the permeate solution as is reflected in Fig.21. As for PA material as shown in Fig.27, the preferential sorption of neither component is predominent. It is assumed in this case that the average value of the preferential sorption is equal to each other. Since the viscosity of hexanol ($\mu = 43.7\ cp$) [51] is 25 times as much as that of ethanol ($\mu = 1.70\ cp$)

at experimental temperature of $23°C$, it is believed that ethanol is more mobile in the interfacial region. The flow of the interfacial layer results in the enrichment of ethanol and the enrichment is enhanced by the higher operating pressure because of more interfacial flow. Fig.21 shows the increased enrichment of ethanol in the permeate product with an increase in the operating pressure.

Fractionation of EtOH-p-xylene feed solution system is the example of the **second** category in which separation decreases with an increase in the operating pressure. Experimental results are shown in Fig.22.

The above results are understandable on the following basis:

1. Ethanol is preferentially sorbed for CAB and PA materials as determined from LC experiments (see Table 5,9).

2. An increase in operating pressure tends to increase the sorption of both preferentially and non-preferentially sorbed components in the interfacial layer. For this mixture, the flow of the interfacial fluid results in the enrichment of the preferentially sorbed ethanol in the permeate product. An increase in the operating pressure leads to an increase in the sorption of both ethanol and p-xylene. As a result of stronger sorption, the mobility of ethanol molecules decreases more than that of p-xylene. Thus the flow of interfacial fluid under higher pressure reduces the enrichment of ethanol in the permeate product. This tendency is reflected in Fig.22.

n-Heptane-p-xylene feed solution falls into the **third** category in which the separation is hardly affected within the operating pressure range from 3448 kPag (500 psig) to 5172 kPag (750 psig) as shown in Fig.23. This is the case which lies between category one and category two. In this

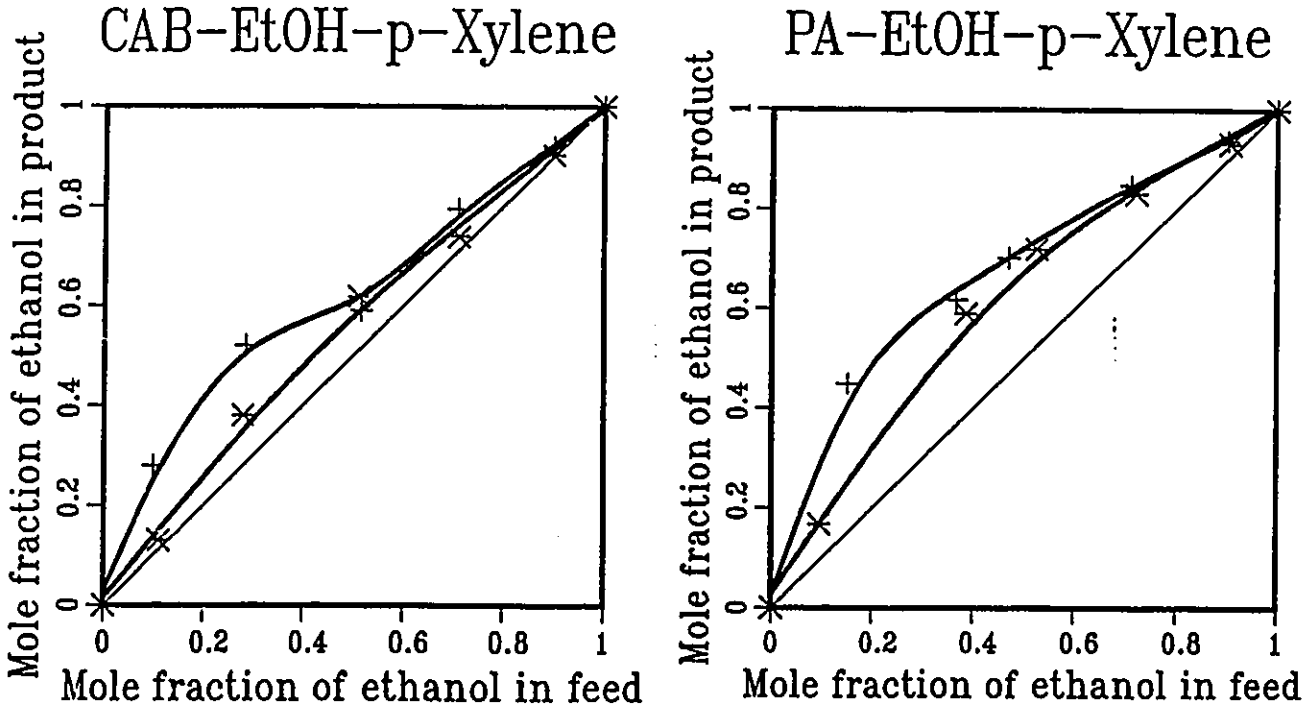

Figure 22: Effect of pressure on RO separation for CAB-EtOH-p-xylene and PA-EtOH-p-xylene systems corresponding to RO data given in Table 3,[1], film No.3 and 11. Legend for operating pressure: +, 3448 kPag (500 psig); *, 5172 kPag (750 psig).

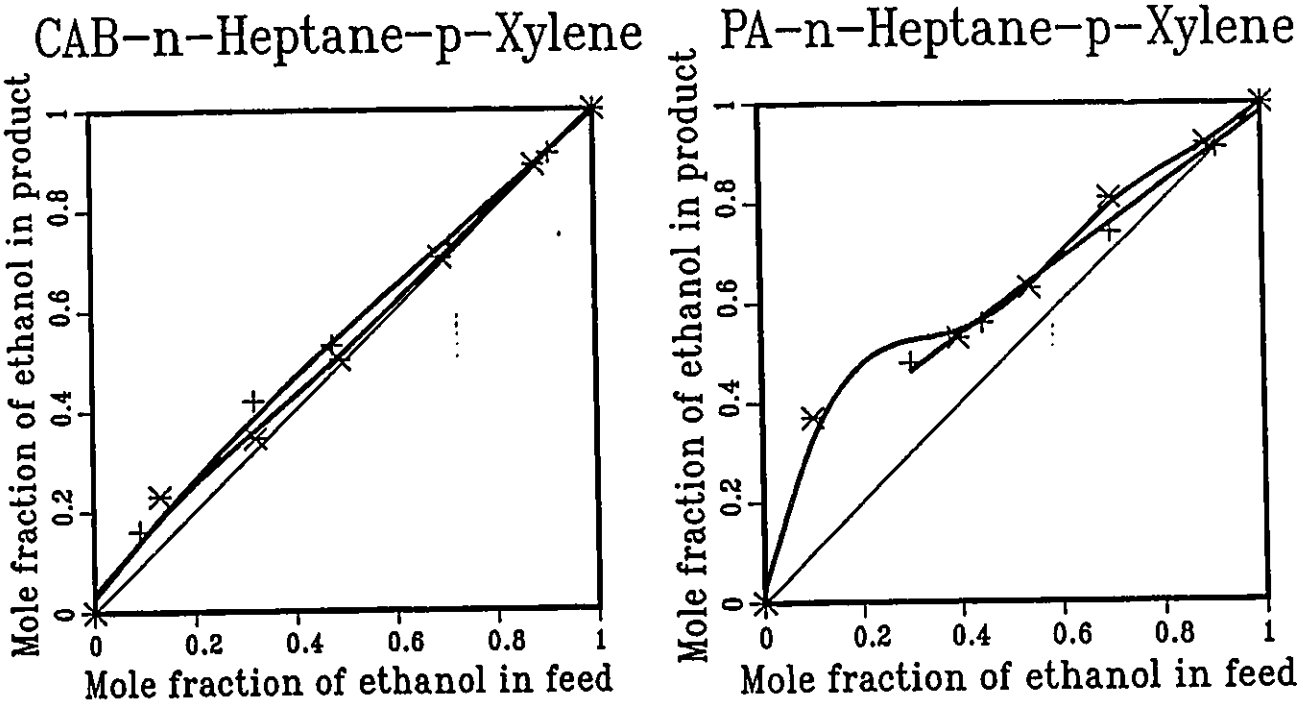

Figure 23: Effect of pressure on RO separation for CAB-n-heptane-p-xylene and PA-n-heptane-p-xylene systems corresponding to RO data given in Table 3,4, film No.8 and 15. Legend for operating pressure: +, 3448 kPag (500 psig); *, 5172 kPag (750 psig).

case, n-heptane is the preferentially sorbed component as determined from LC experiments (refer to Table 7,11). When operating pressure increases, the mobility increase of preferentially sorbed heptane resulting from the pressure increase is well balanced by the mobility decrease resulting from the increase in sorption strength. So is the situation for xylene. Thus the mobility of either component in the interfacial layer remains unchanged or equally changed in the same direction. This accounts for the experimental results.

To summarize, the effect of operating pressure on the degree of separation depends on the preferential sorption of the species, strength of the sorption, and the difference in the mobility of the sorbed species under the conditions of the experiment.

As for the flux of the permeate product through both CAB and PA membranes, there is a general tendency of flux increase corresponding to the increase in the operating pressure, which is understandable on the basis that with an increase in the operating pressure, both the flux of interfacial fluid and that of bulk fluid increase. Therefore, the flux of the permeate solution increases. The product rate data reflect the above tendency.

Fig. 24 illustrates the RO fractionation performance of CAB membrane-EtOH-n-heptane feed solution system for the same CAB membrane with a 30 days' interval.

The data show that while the flux of membrane permeate product solution declined after 30 days' continuous contact with EtOH-n-heptane mixture, the degree of fractionation remained almost unchanged. The results suggest that separations are essentially unaffected by decrease in flux due

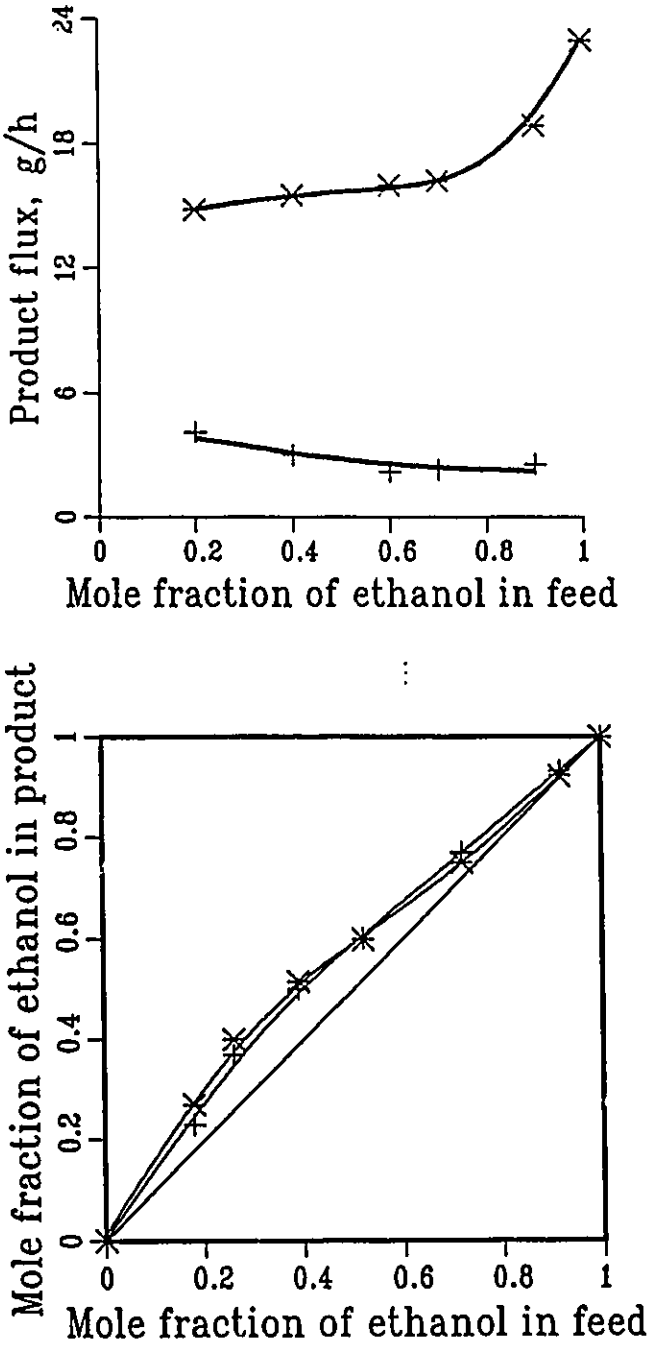

Figure 24: Effect of contact time on RO performance for CAB-EtOH-n-heptane system under operating pressure of 3448 kPag (500 psig) with the same membrane. Legend: *, new CAB membrane; +, CAB membrane with a time interval of 30 days. New CAB membrane has NaCl separation rate of 84.5% with 3500 ppm NaCl-water feed at 1724 kPag (250 psig).Effective membrane area is 9.6 cm^2.

to the collapse of porous substructure of membrane. This shows a direction in the development of membranes for nonaqueous liquid mixture fractionation. While the surface layer should have a sufficient permselectivity, the porous sublayer needs to be sufficiently resistant to organic solvent.

Effect of average pore size on the fractionation

In principle, the mobility of the preferentially sorbed component decreases as the membrane surface, or pore wall, is approached as illustrated in Fig.19; and at any given pressure, decrease in membrane pore size decreases the effective area available for the flow of the bulk fluid, which should increase the net effect of the flow of the interfacial fluid on the separation. The effect of average pore size on RO fractionation is well illustrated in the following two examples.

The first example involves the increase in the separation with a decrease in the average pore size on the membrane surface. Typical examples are shown in Table 4. Referring to PA films 9 and 10, the pore size of film 10 is smaller than that of film 9, as indicated by the higher sodium chloride separation of film 10. Referring further to the separation data of ethanol/n-heptane mixtures by the above membranes, concentrations of ethanol in the permeate from film 10 are higher than those from film 9. This example can be explained by the above general principles.

Heptane is the preferentially sorbed component in this system. A decrease in the pore size results in a decrease in the mobility of the preferentially sorbed heptane molecules in the sorbed region. Thus, the mobility of ethanol relatively increases in the interfacial region. When the pore size decreases, the contribution of the interfacial fluid to total flow increases.

Consequently, the enrichment of ethanol in the permeate solution increases.

The second example involves the decrease in the separation with a decrease in the average pore size on the membrane surface. Typical examples are shown in Table 3. Referring to CAB films 7 and 8, the pore size of film 8 is smaller than that of film 7, as indicated by the higher sodium chloride separation of film 8. Referring further to the separation data of n-heptane/p-xylene mixtures by the above membranes, concentrations of n-heptane in the permeate from film 8 are lower than those from film 7. The above result is also understandable by applying the same principle mentioned above.

For CAB membrane-n-heptane-p-xylene system, heptane is preferentially sorbed in the interfacial layer. A decrease in pore size results in a decrease in the mobility of the preferentially sorbed heptane molecules in the sorbed region. Thus, the mobility of xylene relatively increases in the interfacial region. When the pore size decreases, the contribution of the interfacial flow to the total flow increases. Consequently, the enrichment of heptane decreases in the membrane permeated solution.

The above two examples show that the effect of average pore size on the membrane surface can increase or decrease the enrichment of certain species.

In Fig. 25, the results from PA and CAB membranes are compared. It is interesting to note that, whereas sodium chloride separation by CAB membrane is higher, the separation of EtOH/n-heptane mixtures is higher with PA membranes.

The foregoing discussion clearly demonstrates that the operating pres-

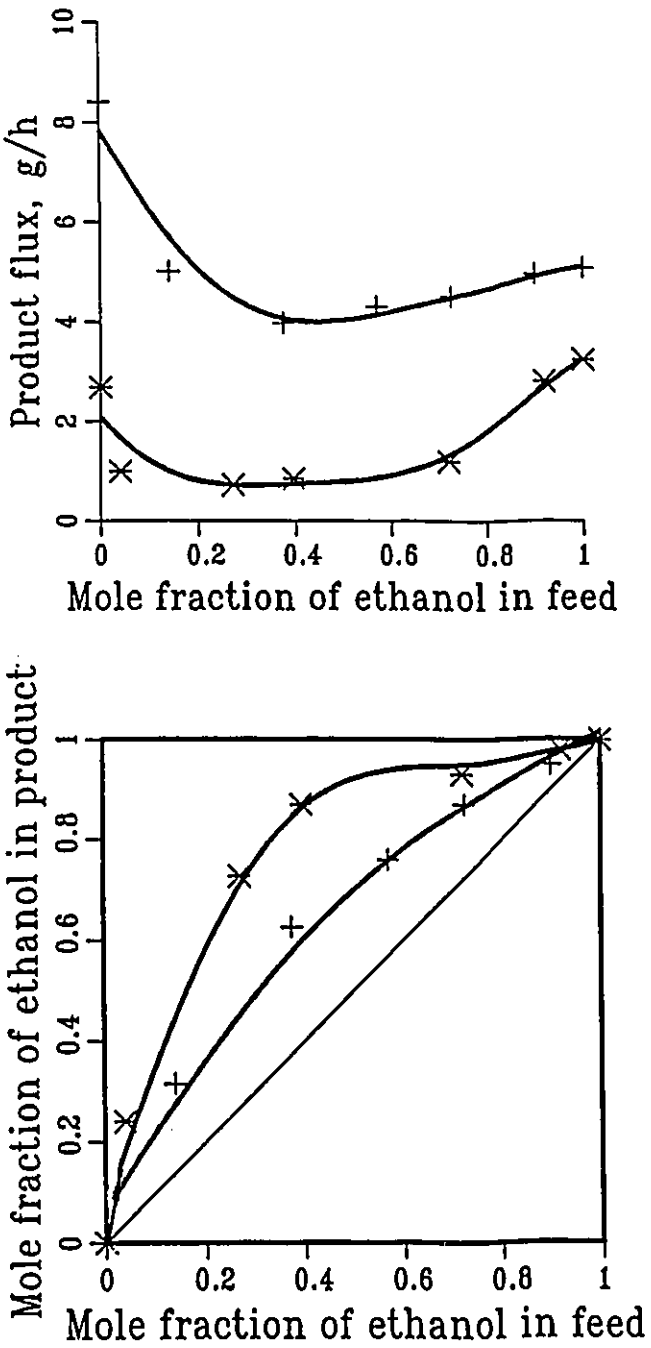

Figure 25: Comparison of CAB and PA RO performance data for EtOH-n-heptane system at 5172 kPag (750 psig). Legend: +, data from CAB membrane with NaCl separation rate of 94.5%; *, data from PA membrane with NaCl separation rate of 92.9%. NaCl separations are tested with 3500 ppm NaCl-water solution at 1724 kPag (250 psig). Data source: Table 3,4 film No.1 and 10.

sure and average pore size on the membrane surface are two important factors controlling the fractionation process. Their variations can positively or negatively influence the extent of the fractionations of binary organic liquid mixtures. Their effect should be carefully considered in the process design as to achieve a desirable direction.

6.2 Preferential Adsorption of Liquid Components to the Polymeric Materials

The Gibbs equation relating interfacial tension (γ) of a solution and the surface excess (Γ) of a solute at an interface can be given in the form [46]:

$$\Gamma = -\frac{1}{RT}[\frac{\partial \gamma}{\partial lna}]_{T,P} \tag{39}$$

where R is the gas constant, T is absolute temperature and a is activity of the solute. Gibbs equation predicts the possible existence of a steep concentration gradient at the interface. Such a concentration gradient at an interface in effect constitutes preferential sorption of one of the constituents of the solution at the interface.

The values of $\Gamma_A A_P \overline{V}_A$ calculated from eq.35 for four binary organic liquid mixtures for CAB and PA material are presented in Table 5-12. They are shown in Fig.11-18. The results show the following preferential sorption characteristics at the polymer-solution interface depending on the solution composition.

The results in Table 13-14 indicate that, for CAB and PA material, one component is preferentially sorbed in the **entire** range of concentrations

Table 13: CAB material sorption characteristics

System A-B	Preferentially sorbed component	Highest sorption at
EtOH-p-xylene	EtOH, $0 < X_A < 1.0$	$X_A = 0.40$
n-heptane-p-xylene	heptane, $0 < X_A < 1.0$	$X_B = 0.40$
EtOH-n-heptane	heptane, $0 < X_A < 1.0$	$X_A = 0.70$
EtOH-1-hexanol	EtOH, $0 < X_A < 0.52$ hexanol, $0.52 < X_A < 0.58$ EtOH, $0.58 < X_A < 1.0$	$X_A = 0.72$

Table 14: PA material sorption characteristics

System A-B	Preferentially sorbed component	Highest sorption at
EtOH-p-xylene	EtOH, $0 < X_A < 1.0$	X_A=0.75
n-heptane-p-xylene	heptane, $0 < X_A < 1.0$	X_A=0.50
EtOH-n-heptane	heptane, $0 < X_A < 1.0$	X_A=0.75
EtOH-1-hexanol	hexanol, $0 < X_A < 0.63$ EtOH, $0.63 < X_A < 1.0$	X_A=0.50 highest negative X_A=0.90 highest positive

in the three binary mixtures, namely, EtOH-p-xylene, n-heptane-p-xylene and EtOH-n-heptane. As for CAB material-EtOH-1-hexanol system , despite the existence of a narrow range of compositions ($0.52 < X_A < 0.58$) where neither component is preferentially sorbed or 1-hexanol is slightly more adsorbed at the polymer-solution interface, ethanol is generally preferentially adsorbed. As for PA material-EtOH-1-hexanol system, in the range of smaller ethanol mole fraction ($0.0 < X_A < 0.50$), 1-hexanol is preferentially adsorbed, while in the range of greater ethanol mole fraction ($0.50 < X_A < 1.0$), ethanol is preferentially adsorbed.A similar change in the adsorption characteristics has been reported by Sourirajan and Matsuura [7]. These results are the reflection of the nature of the polymer-solution interaction, which can be generalized in the following order in the adsorption strength of CAB and PA materials,

adsorption strength: $p - xylene < ethanol < n - heptane$

The above information on the preferential adsorption when combined with information of mobility of component molecules enables one to predict which component is enriched in the membrane permeate product solution without running RO experiments [50].

6.3 Comparison of Membrane Separation Data with Preferential Adsorption Data from LC Experiments

Liquid Chromatography experiments can provide a guideline for determining which species in a binary mixture will be enriched without running RO experiment. Subsequently LC data can determine whether the mem-

brane material is appropriate for the separation of a given solvent mixtures. It may also save a significant amount of time and effort which is needed to make the polymer into a RO membrane when an unsuitable membrane material is encountered. In the following discussions, preferential adsorption data from LC experiments will be compared with membrane separation data and the agreement between them will be examined.

It is generally agreed that RO separation is the combined effect of two factors, namely, (i) an equilibrium effect which is concerned with the details of the preferential sorption in the vicinity of the membrane surface, and (ii) a kinetic effect which is concerned with the mobility of one constituent relative to that of the other constituent in solution through the membrane pore. To simplify the analysis, let the surface excess represent the equilibrium factor which is concerned with preferential sorption and let Stokes' Law radius of the penetrant molecules represent the kinetic factor which is concerned the mobility of molecular species through the membrane pore. Since diffusivity and viscosity are considered in determining Stokes' Law radius, such assumption is reasonable. Therefore, RO separation becomes the combined effect of two factors, namely, surface excess and Stokes' Law radius. Subsequently, one is able to predict which constituent in a binary organic liquid mixture will be enriched in the membrane permeated product solution once surface excess data and Stokes' Law radii are available.

To conduct such analysis, Stokes' Law radii are calculated from Stokes' equation and diffusivities necessary for such calculation are estimated by the Wilke-Chang equation. Details of computation are given in Appendix B. The calculation results are tabulated in Table 15.

Table 15: Stokes' Law Radii

A-B	$r_{AB}, (\times 10^{10})m$	$r_{BA}, (\times 10^{10})m$
EtOH-1-hexanol	1.1	2.5
EtOH-p-xylene	1.1	2.3
n-heptane-p-xylene	2.0	1.9
EtOH-n-heptane	1.1	2.5

By definition, a component with the smaller Stokes' Law radius has the higher mobility. Thus, in the four mixture systems, the component with the higher mobility is identified as shown in Table 16. Table 16 also includes the information on preferentially sorbed component of binary mixtures.

Component which is preferentially sorbed and more mobile is expected to be enriched in the membrane permeate product solution. From Table 16, ethanol is both preferentially sorbed and more mobile for EtOH-1-hexanol and EtOH-p-xylene feed solution systems. Thus ethanol is expected to be the enriched component. For the n-heptane-p-xylene feed solution system, although heptane and p-xylene are equally mobile, heptane is expected to be the enriched compound in the membrane permeated product solution since heptane is preferentially sorbed. For EtOH-n-heptane feed solution system, due to the fact that Stokes' Law radii of ethanol in heptane solvent and heptane in ethanol solvent are $1.1 \times 10^{-10}m$ and $2.4 \times 10^{-10}m$, respectively, it is apparent that ethanol molecule is substantially more mobile in the pore than the heptane molecule, and the difference in mobility is enhanced as the pore size decreases. Therefore, the enrichment of ethanol in the membrane permeated product is expected. The above expectations are well confirmed

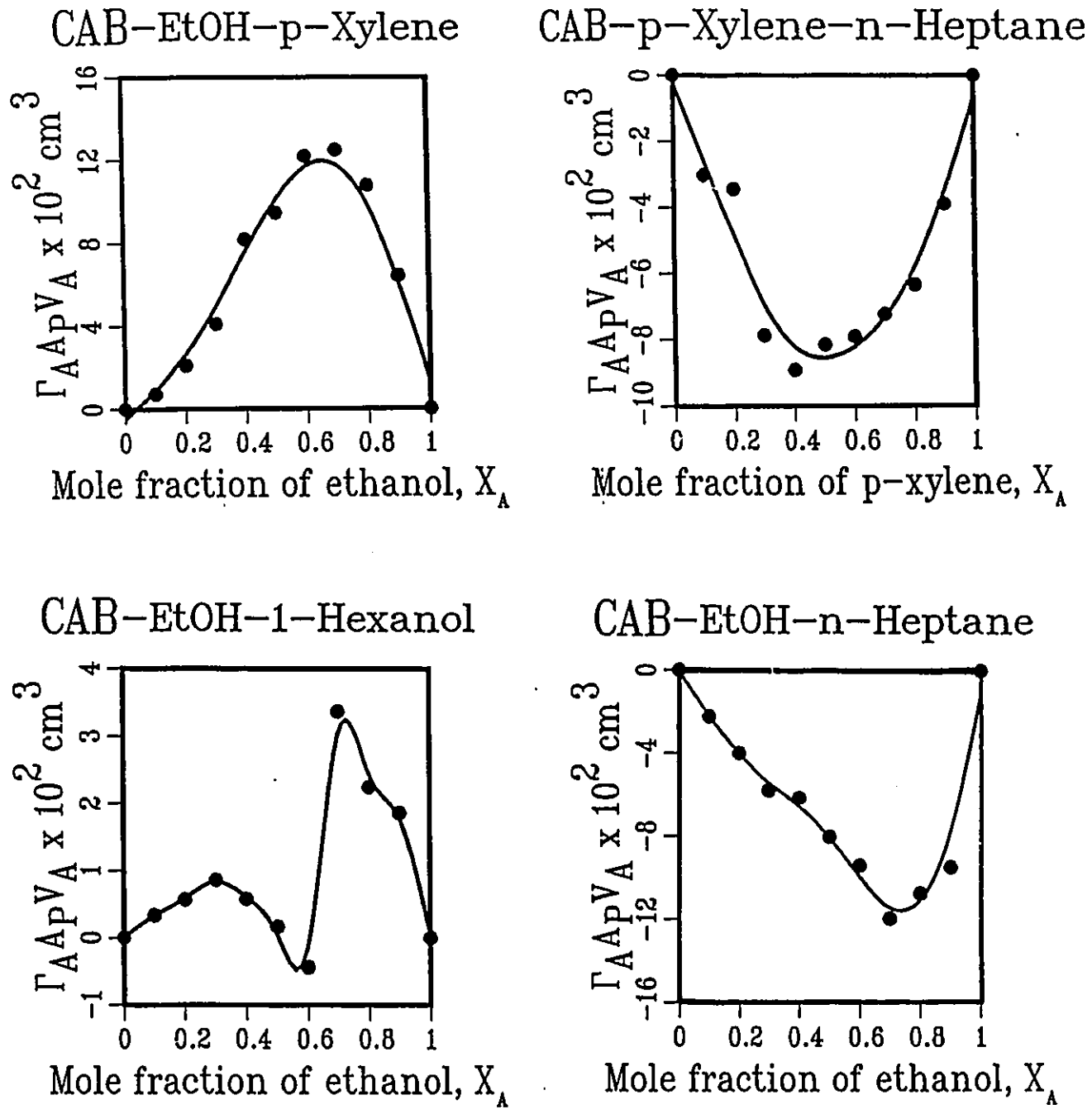

Figure 26: Summing-up of surface excess data for CAB material with 4 mixtures.

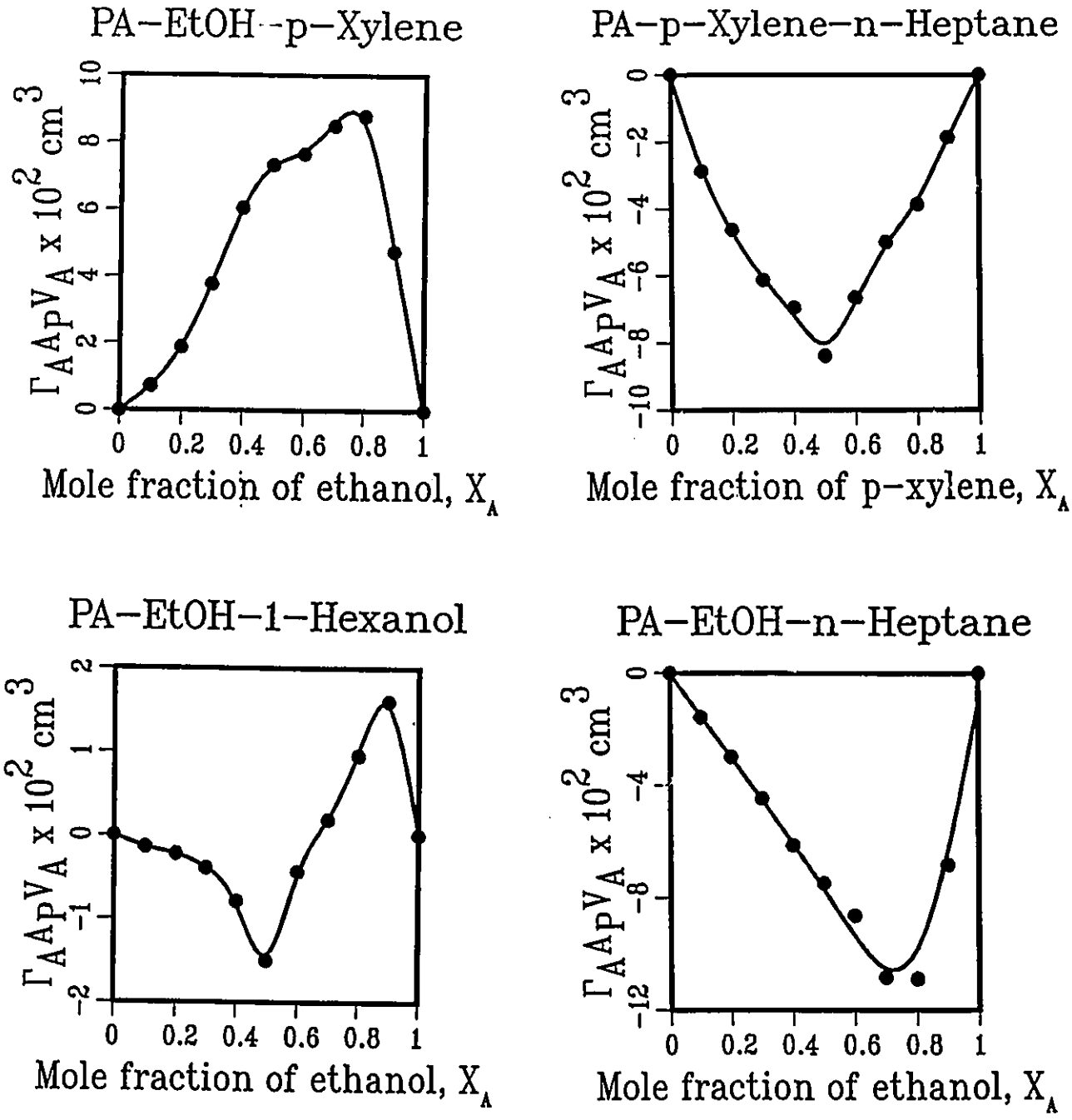

Figure 27: Summing-up of surface excess data for PA material with 4 mixtures.

Table 16: Characteristics of component adsorption and mobility in a binary mixture

A-B	Preferential sorption	More mobile	Expected enrichment[a)]	Actual RO enrichment[b)]
EtOH-1-hexanol	EtOH[c)]	EtOH	EtOH	EtOH
EtOH-p-xylene	EtOH	EtOH	EtOH	EtOH
n-heptane-p-xylene	heptane	equally mobile	heptane	heptane
EtOH-n-heptane	heptane	EtOH	EtOH/heptane	EtOH

a) Refer to component expected to be enriched in membrane permeate product solution.

b) Refer to component actually enriched in RO experiment.

c) For CAB material, EtOH is preferentially sorbed; for PA material, EtOH becomes preferentially sorbed when EtOH mole fraction ranges from 0.63 to 1.0.

by the RO experimental results.

The agreement obtained above with respect to CAB and PA membrane materials are significant from several points of view. They establish the essential validity of the criterion of predicting the component expected to be enriched in the membrane permeated product solution, that liquid chromatography data provides preferential sorption charateristics and that Stokes' Law radius is an indication of the mobility of the penetrant molecule. The RO experimental results are understandable entirely on the basis that RO separation is the combined effect of the preferential sorption factor and the penetrant mobility factor.

Based on the foregoing discussion, a pseudo-operating line can be drawn as shown in Fig. 28.

The physical meaning of Figure 28 must be clearly understood. The curve for the adsorption phase is an arbitrary one which means component A is preferentially sorbed on polymer material. This curve can be drawn qualitively from the surface excess data. r_{AB} and r_{BA} refer to Stokes' Law radius of component A in solvent B and component B in solvent A, respectively. When $r_{AB} < r_{BA}$ which means A molecule is more mobile than B molecule in the membrane pore, the enrichment of component A in the membrane permeated product solution is both thermodynamically and kinetically favorable. This enhances the concentration of A in the membrane permeate product solution. A shift in the operating line in the Fig.28 reflects such an increase. EtOH-1-hexanol and EtOH-p-xylene feed solution systems are two typical examples of the case. When $r_{AB} = r_{BA}$ which means molecule A and B are equally mobile in the membrane pore, the operating

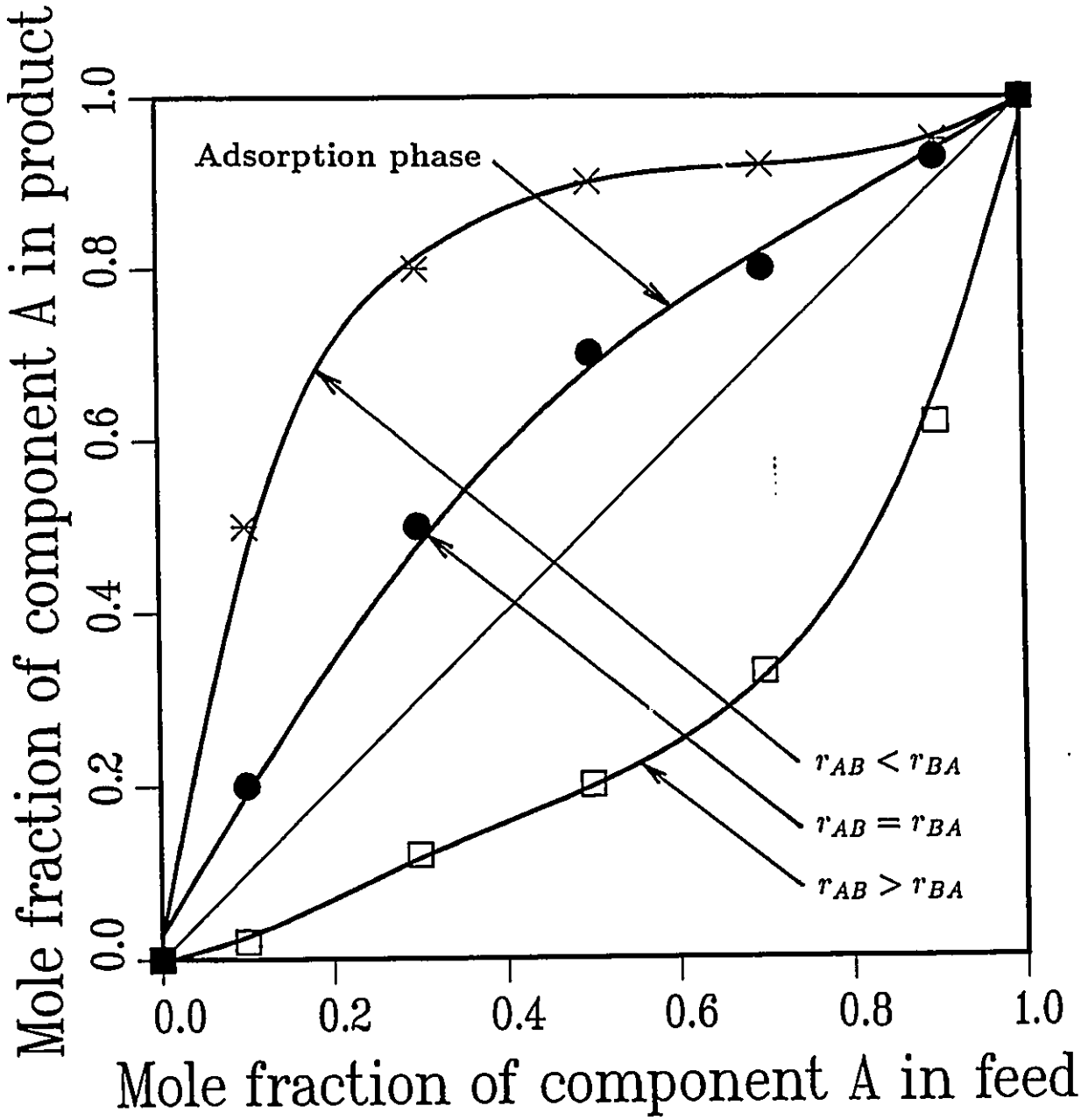

Figure 28: Schematic representation of the pseudo-operating line.

line will be more or less around the adsorption line. n-Heptane-p-xylene feed solution system is an example of this category. Referring to Table 15, Stokes' Law radii for heptane and xylene are almost equal. However, heptane is preferentially adsorbed and subsequently heptane is enriched in the membrane permeated solution. When $r_{AB} > r_{BA}$, especially when r_{AB} is several times as large as r_{BA} , which means the preferentially sorbed component has a much less mobility in the membrane pore, the operating line can be shifted downwards as shown in Fig.28. For EtOH-n-heptane feed solution system, although heptane is preferentially sorbed, Stokes' Law radius of heptane, 2.4 $\times 10^{-10} m$, is two times as large as that of EtOH, 1.1 $\times 10^{-10} m$. Therefore ethanol is enriched in the membrane permeate product solution.

The foregoing results and discussions confirm the fact that RO separations are governed not only by the sorption equilibria but also by the relative mobility of the component molecules through the membrane pore. It also shows the validity of the approach that prediction of which component in the binary mixtrue is enriched in the permeate is possible by considering both surface excess and Stokes' radius.

Chapter 7

7 Conclusions

A major contribution of this work is the further demonstration of the general applicability of RO fractionation of organic liquid mixtures and the establishment of the criterion to predict the to-be enriched component in the membrane permeate product solution for a given membrane material. The specific conclusions are:

1. Separation of the binary mixture of organic liquids takes place in all of the membrane-solution systems studied; PA membranes give higher separation than CAB membranes under the same experimental conditions;

2. The operating pressure and the average pore size on the membrane surface are two important parameters controlling the RO separation of binary organic liquid mixtures.

3. Separations are essentially unaffected by a decrease in the flux, which is caused by the collapse of the porous sub-structure of the membrane;

4. Liquid chromatography is a valid technique as a means of surface excess measurement for binary organic liquid mixtures. The surface excess can be positive, negative, or zero depending on the membrane material-fluid system interactions involved. LC data offers an appropriate means of characterizing interfacial properties of membrane materials;

5. Preferential adsorption exists in all the four binary organic liquid mixtures for cellulose acetate butyrate and aromatic polyamide membrane materials;

6. The combined consideration of surface excess data and Stokes' Law radius gives proper qualitative prediction of the constituent which will be enriched in the membrane permeated product solution without running RO experiments.

Chapter 8

8 Recommendations

It is strongly recommended that this work be further continued giving priority to the following subjects.

1. To carry forward an intensive program of R & D to develop high flux-high separation membranes including cellulose acetate butyrate, aromatic polyamide, polyvinyl alcohol, and ionomer membranes for the industrial RO separation of organic liquid mixtures;

2. To develop appropriate methods for determining the surface area of polymeric materials used in the LC column so that LC data on surface excess can be utilized to calculate the interfacial surface force parameter;

3. Analysis of RO data already generated by an appropriate transport model using the interfacial surface force parameters;

4. To confirm the preferential sorption characteristics of the cellulose acetate butyrate and aromatic polyamide materials shown by the liquid chromatography data for the four model organic liquid mixtures, by other independent physico-chemical techniques. Such confirmation will make LC into a standard technique as a means of measuring surface excess.

9 References

1. Keller,G.E., *Separations: New Directions for an Old Field*, AIChE Monograph Series No.17, Volume 83, 1987. American Institute of Chemical Engineers, Washington, 1987.

2. Committee on Chemical Engineering Frontiers, National Research Council, *Frontiers in Chemical Engineering*, National Academy Press, Washington, D.C., 1988.

3. Sourirajan, S., *Nature*, 203, 1348 (1964).

4. Nader, C., and Farnand, B., *Selection of Membranes Materials by Liquid Phase Affinity Chromatography for Naphtha Upgrading*, Energy Research Laboratories Report No. ERP/ERL 83-69 (TR), CANMET, Energy, Mines and Resources Canada, Ottawa, 1983.

5. Taketani, Y., Matsuura, T., and Sourirajan,S., *Separation Science and Technology*, 17(6), 821, 1982.

6. Matsuura, T., and Sourirajan, S., Characterization of Membrane Materials for Reverse Osmosis in *Proceedings of 32nd Canadian Chemical Engineering Conference* Volume 3, pp.1188-1196, Canadian Society for Chemical Engineering, Vancouver, Canada, 1982.

7. Sourirajan, S., and Matsuura, T., *Reverse Osmosis/Ultrafiltration Process Principles*, National Reseach Council Canada, Ottawa, 1985.

8. Kopecek, J., and Sourirajan, S., *Can. J. Chem.* 47, 3467(1969).

9. Kopecek, J., and Sourirajan, S., *Ind. Eng. Chem. Process. Res. Dev.* 9, 5(1970).

10. Adam, W.J., Luke, B., and Meares, P., *J.of Membrane Science.* 13 (1983)127-149.

11. Farnand, B., Talbot, F.D.F., Matsuura, T., and Sourirajan, S., *Proc. 2nd Bioenergy R & D Seminar*, pp179-183, National Research Council Canada, Ottawa, 1980.

12. Farnand, B., Talbot, F.D.F., Matsuura, T., and Sourirajan, S., *Proc. 4th Bioenergy R & D Seminar* pp.535-539, National Research Council Canada, Ottawa, 1982.

13. Farnand, B., Talbot, F.D.F., Matsuura, T., and Sourirajan, S., *Proc. 5th Canadian Bioenergy Seminar*, pp.195-200, Elsevier, 1984.

14. Kulkarni, S.S., Funk, E.W., and Li, N.N., *Recent Advances in Separation Techniques-III*, N.N. Li(ed.) Symposium Series No.250, Volume 82, American Institute of Chemical Engineers, 1986.

15. King, C.J., Mavratil, J.D., *Chemical Separations* Vol.II, Applications, p.239, Litarvan Literature, Denver & Vienna, 1986.

16. Martin, E.C., Binning, R.C., Adams, L.M., and Lee, R.J., US Patent 3,140,256 (1964).

17. Tadashi, U., Yasuhiro, S., and Mizuho, S., *Separation Science and Technology*, 17(2), 307 (1982).

18. Wan, W., Eur.Pat.Appl. EP 145,127 (1985).

19. Hafez, M. M., and Koenitzer, B.A, Eur.Pat.Appl. EP 137,698 (1985).

20. Chang,Y.A., Kulkarni, S.S., and Funk, E.W., US Patent 4,595,507 (1986).

21. Farnand, B., Ph.D. Thesis, Chemical Engineering Department, University of Ottawa, Ottawa, 1983.

22. Black, L.E., and Boucher, H.A., Eur.Pat. Appl. EP 160,140 (1985).

23. Thompson, J.A., U.S.Patent 4,715,960 (1987).

24. Wernick, D.L., U.S.Patent 4,541,972 (1985).

25. Matsui, K., Ishihara, K., Shinohara, I., Nishide, H., and Kogure, R., Eur. Pat.Appl. EP254,359 (1986).

26. Bitter, J.G.A., and Haan, J.P., Eur. Pat. Appl.EP 254,359 (1988).

27. Mazid, M.A., Review: Mechanisms of Transport Through Reverse Osmosis Membranes, in *Sep. Sci. Tech.*, 19, 357 (1984).

28. Kedem, O., and Katchalsky, A., Thermadynamic Analysis of the Permeability of Biologic Membranes to Nonelectrolytes, in *Biochem.Biophys. Acta*, 27,229(1958).

29. Lui, A., M.A.Sc. Thesis, Chemical Engineering Department, University of Ottawa, 1988.

30. Lonsdale, H.K., Merten, U., and Riley, R.L., *J. Appl. Polymer Sci.*, 9,1341 (1965).

31. Jonsson, G., and Boesen, C.E., *Desalination* 17,145(1975).

32. Matsuura, T., and Sourirajan, S., Reverse osmosis transport through capillary pores under the influence of surface forces, in *Ind. Eng. Chem. Process. Res. Dev.*, 20, 273(1981).

33. Matsuura, T., and Taketani, Y., and Sourirajan, S., Chap.19, in *Synthetic Membranes*, A.F.Turbak (ed.), ACS Symposium Series, American Chemical Society, Washington, D.C., 1981.

34. Chan,K., Matsuura,T., and Sourirajan, S., *Ind. Eng. Chem., Prod. Res. Dev.* 21, 605 (1982).

35. Mehdizadeh, H., and Dickson, J.M. *J. Membrane Science*, 42, 119 (1989)

36. Tam.C.M., personal communcation

37. Schoenmakers, P.L., Optimization of Chromatographic Selectivity: A Guide to Method Developoment, in *J. of Chromatography Library*, Volume 35, Elsevier, 1986.

38. Paris, N.A., Instrumental Liquid Chromatograpy–A Practical Manual on HPLC Methods, in *J. of Chromatography Library*,Volume 27, 2nd edition, Elsevier, 1981.

39. Gutman, R.G., *Membrane Filtration – The Technology of Pressure-Driven Crossflow Process*, IOP Publishing Ltd., 1987, p.16.

40. Matsuura, T., unpublished paper.

41. Matsuura, T., Taketani, Y., and Sourirajan, S., Interfacial parameters governig reverse osmosis for different polymer material-solution systems through gas and liquid chromatography data, in *J.of Colloid and Interface Science*, 95(1), 10, 1983.

42. Huber, J.F.K., and Gerritse, R.G., Evaluation of dynamic gas chromatography methods for the determination of adsorption and solute isotherm, in *J. of Chromatography*, 95(1), 137, 1971.

43. Mohlin, U-B., and Gray, D.G., Gas chromatography on polymer surface adsorption on cellulose, in *J. of Colloid and Interfacial Science*,47(3), 747, 1974.

44. Sourirajan, S., *Reverse Osmosis*, Logos Press Ltd.,2nd impression (1971).

45. Sourirajan, S., *Lectures on Reverse Osmosis*, Division of Chemistry, National Research Council Canada, Ottawa, 1983, p.39.

46. McBain, J.W., *Colloid Science*, p.55, D.C.Heath and Co., Boston, Mass., 1950.

47. Perry, R.H., *Chemical Engineers Handbook*, 5th edition, p.3-234, New York, MaGraw-Hill, Inc.

48. Sourirajan, S., *Lectures on Reverse Osmosis*, Division of Chemistry, National Research Council Canada, Ottawa, 1983, p.318.

49. Matsuura, T., and Sourirajan, S., Material sicence in reverse osmosis and ultrafiltration in *Reverse Osmosis and Ultrafiltration*, ACS Symposium series, the American Chemical Society, Washington, D.C., 1985.

50. Zhou, Q.H., M.A.Sc. Thesis, Department of Chemical Engineering, The University of Ottawa, 1990.

51. *International Critical Tables of Numerical Data, Physics, Chemistry and Technology*, 1st ed., McGraw-Hill Book Company Inc., New York, 1930.

Appendix

A Sample Calculation of Surface Excess

For CAB-EtOH-n-heptane system, known property data:

$\overline{V}_A$ = molar volume of ethanol = M/ρ = 46.07/0.789 = 58.390 cm^3/mol;

$\overline{V}_B$ = molar volume of heptane = M/ρ = 100.20/0.684 =146.491 cm^3/mol;

From LC experiments:

When solvent stream flowrate = 0.30 mL/min,

with known ethanol mole fraction = $x_{A,b}$ = 0.40,

recorded retention times for ethanol, T_A = 4.997 minutes;

for heptane, T_B = 6.233 minutes.

Noting retention volume = flowrate x retention time, and substituting known values into equation 35:

$$\Gamma_A A_P V_A = \frac{(0.4)(58.390)(146.491)(0.30)(4.997-6.233)}{((0.40)(58.390)+(1-0.40)(146.491))^2}$$

$$= -6.150 \times 10^{-2} cm^3$$

Similarly, other surface excess values are calculated.

Appendix

B Calculation of Stokes' Radius

To calculate the Stokes' Law radius, the diffusivity term is first estimated by the Wilke-Chang equation [47] and then Stokes' Law radius is calculated from the Stokes equation [48].

The Wilke-Chang equation is:

$$D_L\mu/T = 7.4\times10^{-8}(XM)^{0.5}/V_b^{0.6} \tag{40}$$

where D_L= diffusivity of solute at infinite dilution,cm^2/sec; μ = solution viscosity, centipoise; T= absolute temperature, K; X=association parameter; M=solvent molecular weight; V_b=molar volume of solute at normal boiling point, cm^3/mol.

Unit conversion factor used in the calculation is:

$1\frac{(cm^2)(cp)}{(s)(K)} = (1\times10^{-4}m^2)[1\times10^{-3}(Newton)(s)/m^2]/[(s)(K)] = 1\times10^{-7}\,Newton/K$

From literature [47]:

solvent	X
ethanol	1.5
p-xylene	1.0
n-heptane	1.0
hexan-1-ol	1.0

All physicochemical properties necessary for the calculation of diffusivity by eq.40 are listed in Table 17.

Table 17: Property Data for the Wilke-Chang Equation

solvent	X	M (g/mole)	$V_b(cm^3/mole)^{a)}$
ethanol	1.5	46.07	59.2
n-heptane	1.0	100.20	162.8
p-xylene	1.0	106.16	140.6
1-hexanol	1.0	102.17	162.8

a) V_b is obtained from the literature [47].

The Stokes equation is:

$$D_L = \frac{kT}{6\pi\mu r_{AB}} \tag{41}$$

where k,T, μ and r_{AB} are the Boltzmann constant, absolute temperature, solvent viscosity and the solute radius respectively.

Rearranging:

$$r_{AB} = \frac{k}{6\pi(D_L\mu/T)_{AB}} \tag{42}$$

Details of calculation are presented as follows.

EtOH-n-heptane system: A=EtOH, B=heptane

For ethanol (A) in solvent heptane (B):

$M = M_{solvent}$ =100.20, $V_b = (V_b)_{solute}$ =59.2, X=1.0 (heptane is solvent)

From the Wilke-Chang equation:

$$\begin{aligned}(D_L\mu/T)_{A\ in\ B} &= 7.4\times10^{-8}[(1.0)(100.20)]^{0.5}/(59.2)^{0.6} \\ &= 6.401\times10^{-8}\frac{(cm^2)(cp)}{(s)(K)} \\ &= 6.401\times10^{-15}\ Newton/K\end{aligned}$$

Substituting into expression for r_{AB}:

$r_{AB} = \frac{1.38048 \times 10^{-23} Joule/K}{(6)(3.1416)(6.401 \times 10^{-15} N/K)} = 1.1 \times 10^{-10} m$

For heptane (B) in solvent ethanol (A):

$M = M_{solvent}$ =46.07, $V_b = (V_b)_{solute}$ =162.8, X=1.5 (ethanol is solvent)

$$\begin{aligned}(D_L\mu/T)_{B\ in\ A} &= 7.4\times10^{-8}[(1.5)(46.07)]^{0.5}/(162.8)^{0.6} \\ &= 2.897\times10^{-8}\tfrac{(cm^2)(cp)}{(s)(K)} \\ &= 2.897\times10^{-15}\ Newton/K\end{aligned}$$

$r_{BA} = 1.38048\times10^{-23}/[(6)(3.1416)(2.897\times10^{-15}] = 2.5\times10^{-10} m$

EtOH-p-xylene system: A=EtOH, B=p-xylene

For EtOH (A) in solvent p-xylene (B):

$M = M_{solvent}$ =106.16, $V_b = (V_b)_{solute}$ =59.2, X=1.0

$$\begin{aligned}D_L\mu/T &= 7.4\times10^{-8}[(1.0)(106.16)]^{0.5}/(59.2)^{0.6} \\ &= 6.589\times10^{-8}\tfrac{(cm^2)(cp)}{(s)(K)} \\ &= 6.589\times10^{-15}\ N/K\end{aligned}$$

$r_{AB} = 1.38048\times10^{-23}/[(6)(3.1416)(6.589\times10^{-15})] = 1.1\times10^{-10} m$

For p-xylene (B) in solvent EtOH (A):

$M = M_{solvent}$ =46.07,$V_b = (V_b)_{solute}$ =140.6, X=1.5

$D_L\mu/T = 7.4\times10^{-8}[(1.5)(46.07)]^{0.5}/(140.6)^{0.6} = 3.164\times10^{-8}\frac{(cm^2)(cp)}{(s)(K)}$

$= 3.164\times10^{-15}\ N/K$

$r_{BA} = 1.38048\times10^{-23}/[(6)(3.1416)(3.164\times10^{-15})] = 2.3\times10^{-10} m$

EtOH-1-hexanol system: A=EtOH, B=1-hexanol

EtOH (A) in solvent 1-hexanol (B):

$M = M_{solvent}$ =102.17, $V_b = (V_b)_{solute}$ =59.2, X=1.0

$D_L\mu/T = 7.4\times10^{-8}[(1.0)(102.17)]^{0.5}/(59.2)^{0.6} = 6.464\times10^{-8}\frac{(cm^2)(cp)}{(s)(K)}$

$= 6.464\times10^{-15}\ N/K$

$r_{AB} = 1.38048\times10^{-23}/[(6)(3.1416)(6.464\times10^{-15})] = 1.1\times10^{-10}m$

1-Hexanol (B) in solvent EtOH (A):

$M = M_{solvent}$ =46.07, $V_b = (V_b)_{solute}$ =162.8, X=1.5

$D_L\mu/T = 7.4\times10^{-8}[(1.5)(46.07)]^{0.5}/(162.8)^{0.6} = 2.897\times10^{-8}\frac{(cm^2)(cp)}{(s)(K)}$

$= 2.897\times10^{-15}\ N/K$

$r_{BA} = 1.3804\times10^{-23}/[(6)(3.1416)(2.897\times10^{-15})] = 2.5\times10^{-10}m$

n-Heptane-p-xylene system: A=heptane, B=xylene

Heptane (A) in solvent xylene (B)

$M = M_{solvent}$ =106.16, $V_b = (V_b)_{solute}$ =162.80, X=1.0

$D_L\mu/T = 7.4\times10^{-8}[(1.0)(106.16)]^{0.5}/(162.80)^{0.6} = 3.5910\times10^{-8}\frac{(cm^2)(cp)}{(s)(K)}$

$= 3.5910\times10^{-15}\ N/K$

$r_{AB} = 1.38048\times10^{-23}/[(6)(3.1416)(3.5910\times10^{-15})] = 2.0\times10^{-10}m$

Xylene (B) in solvent heptane (A):

$M = M_{solvent}$ =100.20, $V_b = (V_b)_{solute}$ =140.6, X=1.0

$D_L\mu/T = 7.4\times10^{-8}[(1.0)(100.20)]^{0.5}/(140.6)^{0.6} = 3.810\times10^{-8}\frac{(cm^2)(cp)}{(s)(K)}$

$= 3.810\times10^{-15}\ N/K$

$r_{BA} = 1.38048\times10^{-23}/[(6)(3.1416)(3.810\times10^{-15}] = 1.9\times10^{-10}m$

Results of above calculation are tabulated in Table 15.

Table 15 Stokes' Law radii

A-B	$r_{AB},(\times10^{10}m)$	$r_{BA},(\times10^{10}m)$
EtOH-n-heptane	1.1	2.5
EtOH-p-xylene	1.1	2.3
EtOH-1-hexanol	1.1	2.5
n-heptane-p-xylene	2.0	1.9

This is the source of Table 15 in Chapter 6.